uc3m | Universidad Carlos III de Madrid

Aerospace Engineering

2017-2018

Bachelor's Thesis

"MECHANICAL CHARACTERIZATION OF COMPOSITE MATERIALS: FRACTURE ENERGIES"

Pedro López López

Tutor

Jesús Pernas Sánchez

Leganés, October 2018

ABSTRACT

Advanced fields like the aerospace industry have seen in the last years an important increasing use of composite materials for their main structures, thanks to the exceptional physical properties they offer at a low weight. Determining some of their most important properties, such as fracture energies, has a significant economic cost on their development, due to the necessity of performing several experimental tests. This thesis aims at creating some FEM models of tension and compression tests using SIMULIA ABAQUS software, that could be used as a cheaper and faster alternative to those carried out in a laboratory. Experimental data will be used to validate the results, and an analysis discussing the feasibility of the models will be performed considering different studied parameters.

Keywords: Composite materials, FRC, fracture toughness, critical energy, Hashin

CONTENTS

LIST OF FIGURES

LIST OF TABLES

1. INTRODUCTION

This section is devoted to explaining the main reasons that lead to the development of this thesis, the defined goals to be fulfilled while performing it and the properly explained, developed process followed in order to achieve them.

1.1. Motivation

Within the last years, composite materials have been able to rapidly expand its market niche, originally focused on the military and aerospace industries, to a whole new set of applications, which will surely suppose a bright future of the engineering and technology design. Although composite materials have been around us for already a long time (bricks made out of straw and mud used in Ancient Egypt, or the mixture of cement, water and other aggregates known as concrete can be considered the first man-made composite materials) it has been in the last 30 years when these materials have seen its boom in terms of engineering applications. The search for strong but yet, lightweight materials, lead the engineers to develop new materials, which key characteristics, among others, where a high strength and stiffness, while at the same time, reducing its weight: Fiber-reinforced composites were developed. One of the properties defining a composite is that the mechanical and physical characteristics of the new product are normally different from that of the materials that form it. As a result of this, many times a great strength-to-weight ratio is offered, which is something that many industries, especially the aerospace, are interested in.

Fiber-reinforced composite materials (FRC) are made of fibers, known as reinforcing constituent, embedded in a matrix in a given pattern, in order to maximize the desired properties of the composites. Although bonded together, each of the components, fibers and matrix, keep their characteristic physical and mechanical properties, while at the same time, achieving a synergistic combination of them, improving the overall performance of the material.

A high economic cost related to the raw materials and manufacturing, along with

the need to perform multiple mechanical tests in order to define all the properties of these anisotropic materials, has as result the increasing use in the last years of numerical simulations to perform parametric studies by means of different commercial FEA software. The motivation of this thesis is to develop consistent FEM models using SIMULIA ABAQUS to simulate some typical mechanical tests used in laboratories, in order to determine the fracture energies of a given composite laminate.

1.2. Thesis objectives

- Develop several numerical models using a FEA software, to simulate real and tested composite laminates.
- Obtain the fracture energies of the modeled laminates, by means of the available tools in the FEA software.
- Discuss the discrepancies found between the experimental results obtained by the different researchers and those obtained by the simulations. Analyze the possible reasons behind this, based on the taken assumptions during the implementation of the FEM models.
- Determine if the developed methodology conforms an accurate enough technique that can be used in the future for related problems.

1.3. Stages of development

Firstly, a thorough literature research is carried out, in order to have a solid background related to composite materials, their classification according to different criteria, and manufacturing processes. Fracture mechanics and damage mechanisms, especially the branches applied to composites are also investigated for a better understanding of the problems to be studied.

Different numerical models will be then implemented in FEM software, defining the material properties and geometry among other parameters that will be used to simulate some experimental tests.

The implemented models are validated, by means of comparing the results obtained in the simulations with the experimental data obtained by the researchers of interest.

Some parameters of interest will be changed to observe the change in the behavior of the models yielding different results. They will be analyzed and discussed based on the knowledge acquired in the first stage.

Finally, some conclusions about the whole work developed in the thesis will be exposed, along with some ideas that could be used in the future to continue this research.

1.4. Methodology

Thanks to the computational development in the last years, almost every person is able to reduce drastically the amount of time and paperwork complex elasticity and structural analysis problems, especially in aeronautical engineering, needed in the past: Finite Element Method (FEM) allows this type of problems to be numerically solved with a simplified, time- and money cost. FEM is implemented in much commercial software nowadays, each specialized in a given field, such as fluid mechanics, thermodynamics, etc. It will be SIMULIA ABAQUS software, the one used to carry out this thesis.

1.5. Thesis organization

The report of the thesis is to be divided into the following, differentiated sections:

- Section 1: *Introduction*. The topic of the thesis is briefly explained, while at the same time stating the motivation and purpose that lead to the materialization of this project, and the way and means of developing of the thesis.
- Section 2: *Theoretical approach*. An extensive background related to the topic of the thesis is here properly stated, allowing the not familiarized reader to better understand the rest of the project, while at the same time, presenting the current state of the art to those already in touch with the subject.
- Section 3: *Literature survey*. The most relevant theories related to fracture mechanics and damage mechanisms the thesis' work will be based on are here presented, along with their respective formulations.

- Section 4: *Numerical models*. The steps followed for the implementation of FEM models in ABAQUS software based on the experimental research are clearly defined, explaining the decisions and assumptions taken in order to correctly achieve them.

- Section 5: *Results and Discussion*. The implemented FEM models are here tested and firstly validated with those experimentally obtained. An analysis of the results is performed, discussing the effect of different parameters on them and the possible reason behind the observed behavior.

- Section 6: *Socio-economic impact and legal framework*. A budget of the whole project along with the socio-economic and legal impact it supposes is defined in this section. Applicable standards are also mentioned,

- Section 7: *Conclusions and future projects*. Final conclusions achieved at with this project are stated. Future research related to it is also suggested.

2. THEORETICAL APPROACH

In this section, composite materials are defined in detail, allowing for a deep comprehension of their characteristic properties, as well as its main applications in the different fields throughout their history. Some of the current manufacturing processes are also detailed in this section, exposing those more technologically advanced that are used in the industries around the world.

2.1. General definition

'Composite material' can be defined as a combination of (usually) two different materials, each with their own mechanical and chemical properties, that work together after being judiciously embedded, either physically or chemically, producing a new material with unique properties which are, yielding here the main reason for the composite materials to exist, better than the sum of those of the constituent components, thanks to this 'principle of combined action' observed in the produced combination. Many composite materials fit under this definition, both natural (wood, composed of cellulose and lignin) and early-developed (wattle and daub). But it is the fiber-reinforced and structural composites developed for the aerospace industry, the focus of this thesis.

2.1.1. Fiber-reinforced composites

Fiber-reinforced composites (FRC) conform the most important type of composites used in the different technological applications nowadays. The desired goals to be achieved while designing these materials are mainly, a high strength and stiffness while keeping the weight as low as possible. The aerospace industry is therefore especially interested in this type of materials, due to its constant battle with the weight of its products. These properties can be defined using the specific strength (tensile strength-density ratio) and specific modulus (modulus of elasticity-density ratio). A broad division can be done, based on the type of fiber and matrix used:

Fiber	Advantages	Disadvantages
E-glass, S-glass	High strength Low cost	Low strength Short fatigue life High temperature sensitivity
Aramid (Kevlar)	High tensile strength Low density	Low compressive strength High moisture absorption
Boron	High stiffness High compressive strength	High cost
Carbon(AS4, T300, C600)	High strength High stiffness	Moderately high cost
Graphite (GY-70, pitch)	Very high stiffness	Low strength High cost
Ceramic (silicon carbide, alumina)	High stiffness High temperature	Low strength High cost

Figure 2.1: Typical fiber materials and their properties [1]

Polymer-matrix composites

Polymer-matrix composites (PMC) are those consisting of a polymer, reinforcing resin, with fibers as the dispersed phase. Thanks to their low cost of fabrication, and being room temperature the condition they perform best at, PMCs are the most used composites, both in terms of quantity and range of applications.

Depending on the type of fiber used, PMCs can be classified in Glass fiber-reinforced composites, accounting for the most part of the production of PMCs, thanks to their ease to drawn, high specific strength and corrosion resistance. Carbon can also be used for the fiber material, making Carbon-fiber reinforced composites the most commonly found in advanced composite materials. They are used in top fields, such as aerospace and military, thanks to the carbon fibers being the ones with the best specific properties of the available fiber materials. Having an excellent performance at high temperatures also makes carbon the best choice for harsh environments like spacecraft reentry. The third main group within PMCs is called Aramid (ARomatic polyAMIDe) fiber-reinforced composites. The molecules are greatly oriented in the fiber axis, allowing these composites to have the best fiber strength among the different synthetic fibers. Commercialized under the trade names of Kevlar and Nomex, these materials are used in mainly in military applications, such as body armor protection.

Metal-matrix composites

Metal-matrix composites (MMC), changes the polymer by a ductile metal in the matrix composition. Although MMCs offers some interesting improvements over the PMCs, such as inflammability and more demanding operating temperature ranges, their manufacturing cost is significantly greater, reducing their possibilities of uses [24].

The development of superalloys like Inconel and Waspaloy, allowed the scientists to improve their engineering designs thanks to their excellent mechanical strength, resistance to creep deformation, among other key characteristics. But it was found out, that the only use of these materials was not enough for some applications. MMCs were developed for these great demanding situations, using superalloys, as well as other metal alloys (being aluminum alloys the most used) as matrix materials. Along with carbon, silicon carbide or other metals like Boron for the fiber composition, MMCs offers today a high-temperature creep resistance and stiffness choice for environmentally harsh applications, like engine components, as well as more 'civil' ones, like golf clubs.

Ceramic-matrix composites

It is well known that ceramic materials offer a great oxidation resistance at high temperatures but at the cost of brittle fracture weakness. This problem was solved with the development of ceramic-matrix composites (CMCs), embedding together a ceramic matrix with fibers of another ceramic. The result is a high fracture toughness, thanks to the fiber bridging when the matrix cracks, as well as corrosion stability and a great electrical and thermal insulation. All these make CMCs an excellent choice for high-temperature turbine blades, combustion chambers and spacecraft heat shields.

matrix Type	Fiber	Matrix
Polymer	E-glass S-glass Carbon (Graphite) Aramid (Kevlar) Boron	Epoxy Polyimide Polyester Thermoplastics (PEEK, Polysulfone, etc.)
Metal	Boron Borsic Carbon (Graphite) Silicon carbide Alumina	Aluminum Magnesium Titanium Copper
Ceramic	Silicon carbide Alumina Silicon nitride	Silicon carbide Alumina Glass-ceramic Silicon nitride
Carbon	Carbon	Carbon

Figure 2.2: Summary of fiber-reinforced composites [1]

2.1.2. Structural composites

This type of composite materials embraces those composite structures in which the geometrical design of the different elements plays an important role, along with the unique properties of each of them. These homogeneous materials can be set either in a laminar of sandwich disposition.

Laminar composites

Consisting of an assembly of different fiber-reinforced, composite layers, laminar composites offer virtually isotropic properties in a 2D plane, thanks to the different orientations the layers of material are thoughtfully stacked in, yielding a high strength in the distinct directions of the layers. Different materials can be used for the bonded layers, resulting in a synergistic combination of the individual mechanical and chemical properties.

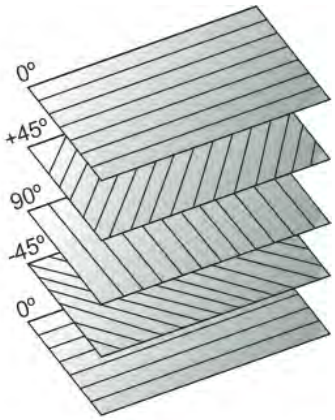

Figure 2.3: Typical orientation of composite layers [2]

Sandwich composites

Resembling the so-called food, sandwich-structured composites are made of two thin layers, known as faces, bonded to a thick, light core placed in-between. Stiff materials like aluminum alloys or carbon fiber-reinforced thermoplastics are used for the faces, giving the structure its high strength, while low-density polymeric foams or honeycombs are used as core material. Aircraft fuselage and space satellites are the high-end technological uses of this type of composite materials [24].

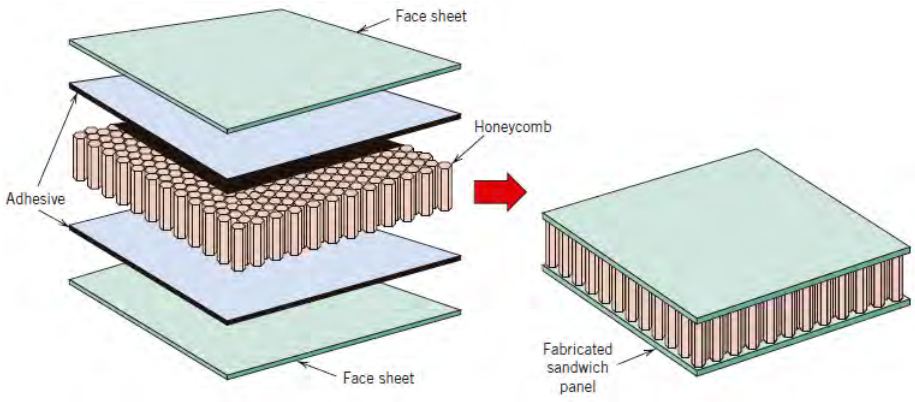

Figure 2.4: Construction of a sandwich panel [3]

2.2. Manufacturing processes

Due to its increasing use in a variety of industries nowadays, the manufacturing of composite materials has developed a wide range of producing processes, depending on the different nature of the elements composing the fibers of matrices of the composites. With the evolution of these processes, better, faster and more efficient ways of manufacturing have been designed in order to satisfy the increasing demand for this materials.

Hand Lay-Up

Being the simplest composite manufacturing method, HLU offers a series of advantages that makes it interesting to the manufacturers: flexible design, making easily large and complex items, while at the same time, it is not needed a huge initial investment as tooling and equipment cost is minimal, and worker training is not demanding. On the other hand, it is a 'traditional' process, meaning the produced volume low, as the prepeg is manually placed on the tool, and required curing times are relatively longer than with other methods. Quality is closely related to the skill of the operator, being the waste factor a relevant reality in case not much care is taken during the layup.

Automated Tape Lay-Up

Thanks to the advanced robotics available today, HLU can be vastly improved by means of automatizing the process. These computed-guided machines are able to quickly produce big flat composite parts, such as airplane wings, with a high productivity rate and precision at the cost of a big initial investment in the purchase of these robots. The automatized process implies that the quality of the final product is no longer linked to the abilities of the operator, allowing for a much more consistent rate of production.

Figure 2.5: ATL machine [4]

Filament Winding

A classic and simple process for manufacturing fiber-reinforced composites. This technique involves winding dry fiber, which has previously been impregnated with a resin bath, on a mandrel which rotates in a variety of orientations, allowing complex shapes to be produced. The process is repeated until the required thickness is achieved, being at this point heat-cured. Mainly used for helicopter blades, cylindrical tanks or tubes, filament winding offer a cheap, fast and very automatized method, while sacrificing the types of available shapes to convex ones, and the possible appearance of delamination or air bubbles, due to a poor fiber bath.

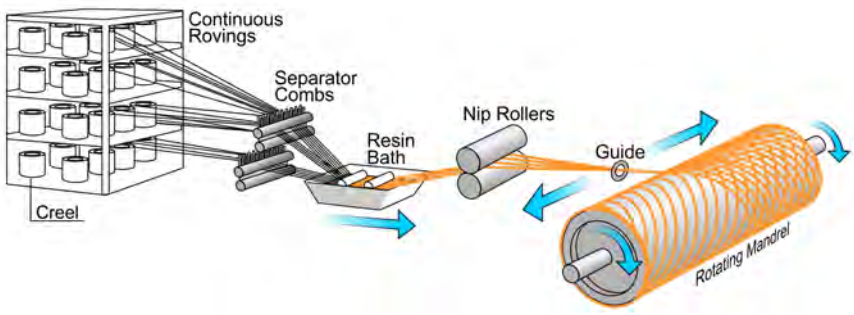

Figure 2.6: Schematic of Filament Winding process [5]

Resin Transfer Molding

RTM process places dry fiber in a closed mold, and then injecting pressurized resin in it, evacuating the air through different vents located along the mold to avoid dry spots. The mixture is then heat-cured, being the curing cycle dependent on the type of used resin and desired thickness, among other parameters. Some of the advantages offered by this manufacturing process are its ability to produce complex shapes with uniform thickness, good surface finish and tolerance accuracy, while at the same time, assuring good mechanical properties and moldability. Regarding the costs, RTM is able to work with much faster cycles than HLU (increasing significantly the productivity), with a reduced importance of the operator skill. As the working pressures are low (around 600 kPa), the tooling cost is reduced in order to meet these not much-demanding pressure conditions. Being a 'mold process' implies that RTM has a critical point in mold design, making efficient and precise tools a must, while at the same time assuring the difficult task of controlling how the resin uniformly flows in the mold.

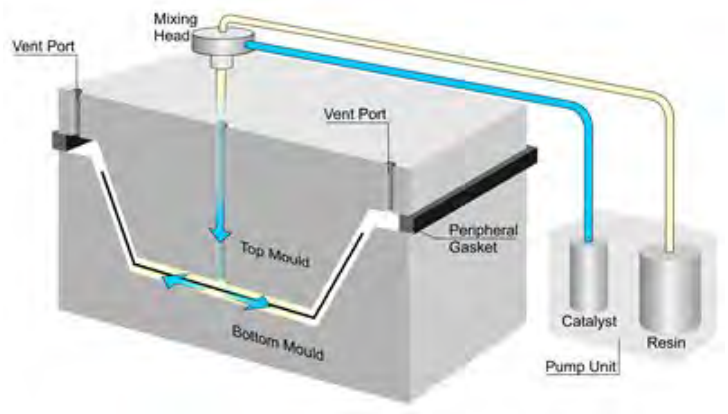

Figure 2.7: Schematic of RTM process [6]

A variation of this method is called Vacuum-Assisted Resin Transfer Molding (VARTM), in which a flexible bag is used to seal the layup. Vacuum is applied after injecting the resin, extracting all the contained air within the fibers.

Pultrusion

When uniform cross-section pieces are needed to be produced, such as beams or hollow tubes, pultrusion is the process used in composite manufacturing. It is closely related to the extrusion process, in which hot metallic rods are pulled through a closed, heated die to achieve the desired shape. The basic process consists of firstly bathing the bundle of reinforcement fibers with resin, stabilizers and fire retardant. The wet fibers are then passed through some performers, getting rid of the excess of resin and assuring the proper distribution of the fibers, and immediately pulled through firstly a forming die, giving the bundle the required form, and then through a heat curing die, in which the fibers are cured and hardened into the final structural product [21].

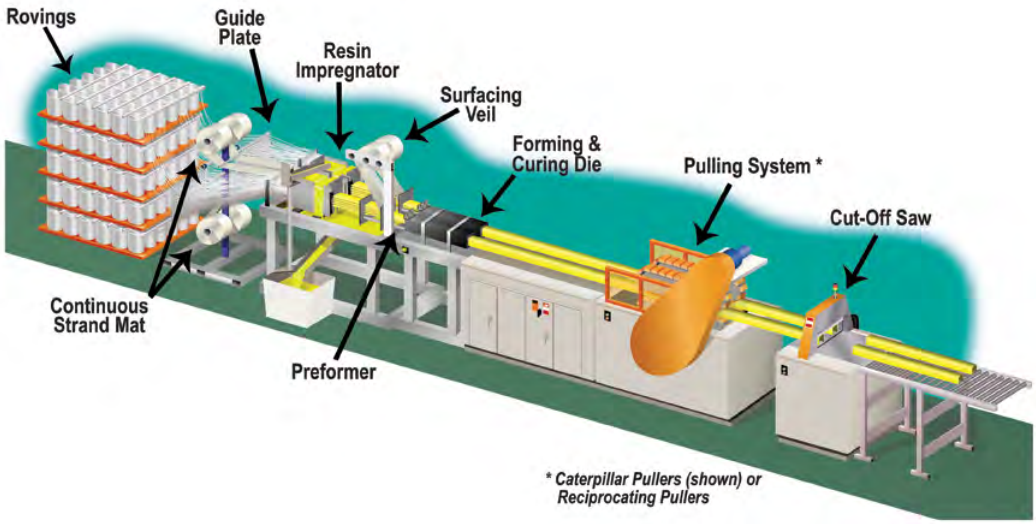

Figure 2.8: Schematic of pultrusion process [7]

Thanks to the natural strength of the used longitudinal fibers, the composite structures obtained with this process offer an exceptional strength and rigidity in their direction. The costs related to the process are also low, as well as the worker skill and possible scrap. The finished products are simply needed to be cut in the required lengths.

2.3. Applications

Marine applications

Composite materials, especially those made of glass fiber-reinforced laminates, have been used in the marine industries shortly since the end of World War II. The timber, which has been the traditional choice for manufacturing boat hulls, was during the first postwar years a scarce and expensive resource. It was then when manufacturers decided to try this newly developed, composite materials. It was found out that composites offer a wide range of advantages compared to the historic materials, such as wood and metal: it is known that marine environment is harsh and highly demanding for structural components, whose properties are easily degraded by the combination of the salty seawater and the different marine organisms. As a result of this deterioration, frequent maintenance is required for repairing the components, which at the end has a high economic cost [20]. Fiber-reinforced composite laminates perform exceptionally in this difficult environment, due to their high corrosive resistance to galvanic and rotting effects. Not only are they more environmentally resistant than traditional materials, but they also offer a higher strength-to-weight ratio, allowing for lighter structures, yielding a more fuel-efficient and cheaper design. Thanks to the different molding processes available, complex, seamless composite structures are easily manufactured.

Early naval applications were related to the military. Huge minesweeper vessels were manufactured using glass-reinforced polymers, taking advantage of its non-magnetic properties to better fulfill their mission, avoiding the danger related to magnetic mines. Submarines have been also improved during the past years thanks to the introduction of composite materials within their construction. Sonar bow domes and submarine fairwater are good examples of large and complex structures made of composites, mainly glass/epoxy panels. Their use allows the Navies around the world to reduce the total weight of the vessel, as well as improving its corrosive resistance compared to the conventional steel components [23].

Competitive racing watercraft is the other main field of marine composite applications. The need for minimizing the weight, in order to have a competitive design, and maximizing the structural stiffness, to ensure the safety of the drivers, makes glass fiber-

reinforced composites the optimal choice for manufacturing racing sailboats, like those seen in America's Cup and drag boat competitions. Their light, stiff and resistant designs allowing these boats to speed up to 400km/h, are only possible thanks to the excellent properties of composite materials.

Figure 2.9: America's Cup vessel with a composites hull [8]

Space applications

Composite materials have been one of the fundamental keys of the space race. Being weight reduction a maximum priority, especially during the launch stages, along with their ability to maintain their mechanical properties over a wide range of temperatures, made the engineers opt for this type of materials, despite the high prices for their manufacturing during the first years. Being the Apollo missions the first ones in which composite materials were introduced, their use in this industry has exponentially grown to the point in which nowadays they are the main component of the different space vehicles.

Space represents the ultimate extreme environment. Vacuum means being exposed to different radiations, which can have significant changes in some of the mechanical properties, such as melting points and tensile strength. As these effects are cumulative, adequate protection is needed for the long radiation exposure. The range of temperatures faced by the space structures range from -100^{o}C to +100^{o}C, known as thermal cycling, is due to their orbital movement around the Earth, being in and out of the Earth's shadow on

a cyclical schedule. Launch and reentry also test to the maximum the thermal capabilities of the structures, as temperatures higher than 1500°C are easily encountered. Atomic oxygen is a major concern for low Earth orbit (LEO) space applications, where non-metal materials were observed to be very reactive to atomic oxygen, which could lead to a fatal disintegration of the affected component. These extremely demanding conditions, along with minimal weight being a must, forced the different engineers to think outside the traditional materials, like steel and titanium [19].

As result, composites reinforced with fibers like carbon and graphite were developed. These advanced composite materials offer a very high specific strength and modulus, while remaining stable in terms of mechanical properties for a wide temperature range, thanks to their low coefficient of thermal expansion. These exceptional characteristics have allowed the design and development of some of the most advanced pieces of human history: the space shuttle uses reinforced carbon-carbon composites for its essential thermal protection system, as well as other parts of its structure. Some advanced telecommunications and scientific satellites, like the XMM-Newton, the biggest satellite developed by the European Space Agency, which relies on ultra-high modulus, carbon fiber composite materials for its main structural elements, guaranteeing the integrity of the spacecraft [18].

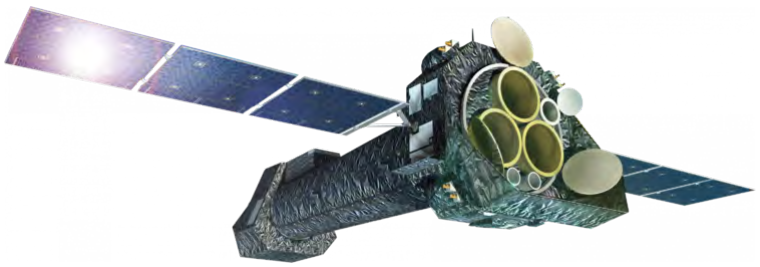

Figure 2.10: XMM-Newton satellite uses carbon composites for its main components [9]

Aircraft applications

Although designed firstly for spacecraft, it is the military and commercial aircraft industries the leading field in which composite materials are used. The possibility of reducing weight in order to increase payload and operational speeds makes composites the logical choice for aircraft manufacturing. They are not only lighter, but in many cases, they are

also stronger and more damage tolerant than the traditional metal structures. Corrosion resistance is also an important advantage with respect to metals, as oxidation plays no role in them. The ease with which composite materials can be molded into the complex shapes required by the different aircraft structures is a positive characteristic as well.

As for much of the advanced technology developed in the last century, composite materials were firstly used in the military aircraft, starting 40 years ago with the design of the American F14 and F15 fighters. During these first years, composites were only used in secondary structures, like the skin empennages of the F15 fighter, manufactured with boron-reinforced epoxies. This was due mainly to the initial phases of investigation composite materials were at that time. As this knowledge increased with the development of new, more advanced composites, its presence in the final configuration of the military aircraft has greatly increased. Good examples are found nowadays in the US F22 fighter, with a 25% of the total weight, mainly with RTM-manufactured composite materials, and within the European market, Eurofighter is the best representation of its increasing application: more than 82% of the airframe is made of composites, being carbon and glass fiber-reinforced materials the ones used, allowing the aircraft to have a highly strong structure, and a very low radar signature, increasing its stealth capabilities [17].

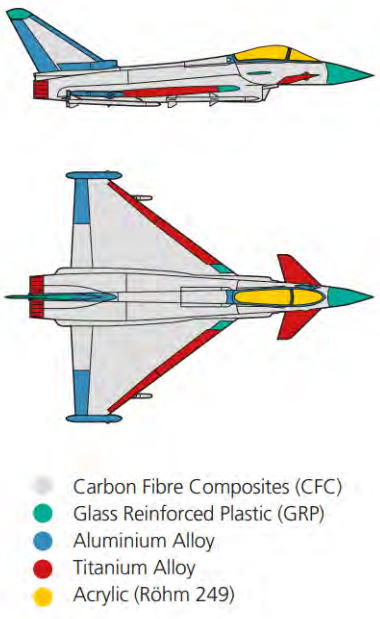

Figure 2.11: Distribution of materials in Eurofighter airframe [10]

Regarding commercial aircraft, the reasons behind the use of composite materials are more related to economics: a lighter airframe means increased fuel efficiency and therefore, reduced operational costs. Since the material does not rust or corrode, repairs and scheduled maintenance are also reduced. Airbus and Boeing manufacturers have spent the last 30 years developing new aircraft designs in which the use of composites has increased with time: starting in 1988, Airbus presented the A320 aircraft with an all-composite tail section, being the same feature also seen in the Boeing 777 designed in 1995 [17]. This 'composites race' has led both companies to their newest designs with more than half of total weight composed solely on advanced composite materials:

The Airbus A350 XWB, made out of a 53% composites, mainly uses carbon fiber-reinforced materials in the fuselage, wing box and empennages. On the other hand, Boeing manufactures the fuselage, wings and most of the airframe components of the Boeing 787 with fiberglass and carbon laminates. Thanks to this broad use, these new aircraft have a stronger, tougher and lighter overall structure, while reducing the costs related to fuel and maintenance.

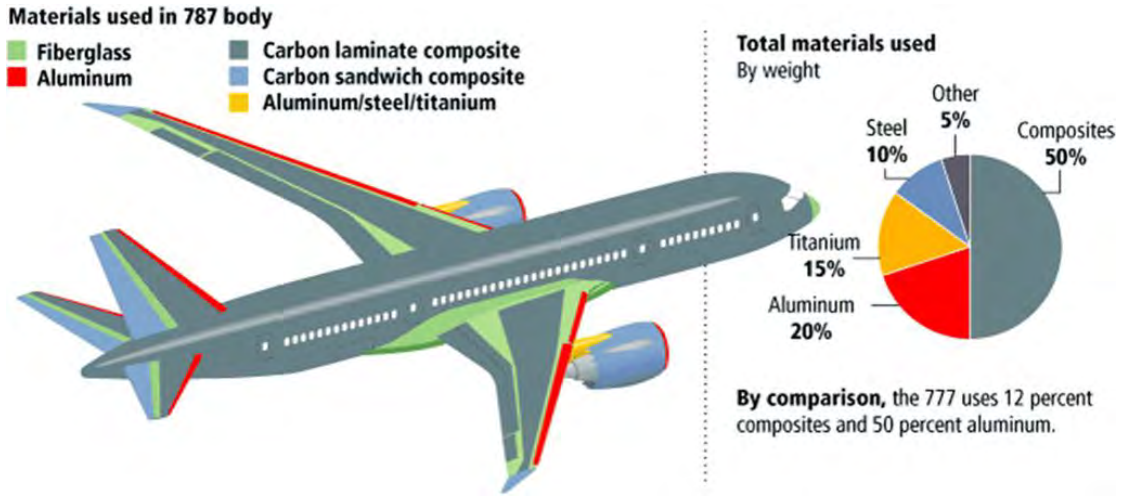

Figure 2.12: Boeing 787 is one of the current commercial aircraft with more composites [11]

3. LITERATURE SURVEY

This section is devoted to briefly explaining the relationship between fracture mechanics and composite materials, due to the characteristic properties of them. The damage model that will be used for the developing of this thesis, along with the way it is implemented in the used FEA software, is also described.

3.1. Composite material behavior

Composites are strongly anisotropic materials. Depending on the direction of load application, the material's response greatly changes. Engineers take advantage of this behavior when designing new composite materials, as a sensible orientation of the fibers forming a laminate can yield a material performance many times better than those traditional, isotropic materials, like metals.

When a load is applied to them, composites show different behaviors depending on their mechanical properties. Prior to the failure load, the response of a composite material can be stated as linear elastic, so classic methods for stress and strain can be used to model it. Thanks to this, standard finite element methods are enough to solve the equilibrium equations affecting the material. Once this critical load is achieved, a failure criterion is to be applied in order to model the post-failure behavior. With the development of composite materials during the last 70 years, many failure criteria have been proposed.

A majority of these criteria can be labeled as 'progressive damage modeling'. These methods study how the overall strength of a laminate will be affected by the propagation of a given damage feature, like a crack. Recalling the basic definition of a composite laminate, each of the layers, differently oriented, will face different stresses, and therefore, individually fail at dissimilar time and ways. Progressive damage models can be used to determine how the laminate properties degrade and when the total failure of it will take place, accounting for the different layer failures [22].

Different material properties are needed in order to completely define each of these failure criteria. There exist some more complex damage models, that yield better and

more accurate results, but on the other hand, require more properties to be stated, reaching a point in which they are almost not practical to be used. All these material properties are to be experimentally determined, which demands an economical and time investment, in order to obtain sufficiently accurate results, using some of the standards produced by The American Society for Testing and Materials (ASTM) for testing procedures. This process is especially tedious regarding composite materials, as, due to their anisotropic behavior, the loading direction is important.

3.1.1. Hashin's Theory

The progressive damage model that will be used in this thesis is criteria developed by Hashin and Rotem in 1973 [27], and later improved by Hashin in 1980 [28]. This model requires the definition of the longitudinal tensile strength, longitudinal compressive strength, transverse tensile strength, transverse compressive strength, longitudinal shear strength and the transverse shear strength of the material to be studied to determine the moment at which damages initiates. Considering four damage initiation mechanisms, fiber tension, fiber compression, matrix tension and matrix compression, the different measured stresses are here compared to the material properties, by mean of the following equations:

Fiber tension ($\hat{\sigma}_{11} \geq 0$):

$$F_f{}^t = (\frac{\hat{\sigma}_{11}}{X^T})^2 + \alpha(\frac{\hat{\tau}_{12}}{S^L})^2 \tag{3.1}$$

Fiber compression ($\hat{\sigma}_{11} < 0$):

$$F_f{}^c = (\frac{\hat{\sigma}_{11}}{X^C})^2 \tag{3.2}$$

Matrix tension ($\hat{\sigma}_{22} \geq 0$):

$$F_m{}^t = (\frac{\hat{\sigma}_{22}}{Y^T})^2 + (\frac{\hat{\tau}_{12}}{S^L})^2 \tag{3.3}$$

Matrix compression ($\hat{\sigma}_{22} \geq 0$):

$$F_m{}^t = (\frac{\hat{\sigma}_{22}}{2S^T})^2 + [(\frac{Y^C}{2S^T})^2 - 1]\frac{\hat{\sigma}_{22}}{Y^C} + (\frac{\hat{\tau}_{12}}{S^L})^2 \tag{3.4}$$

The meaning of the variables of the previous equations is: X^T (longitudinal tensile strength), X^C (longitudinal compressive strength), Y^T (transverse tensile strength), Y^C

(transverse compressive strength), S^L (longitudinal shear strength) and S^T (transverse shear strength), properties of the material. α coefficient determines the contribution of the shear stress to the fiber tensile initiation criterion, and $\hat{\sigma}_{11}, \hat{\sigma}_{22}, \hat{\tau}_{12}$ are the components of an effective stress tensor.

3.1.2. FEM implementation

In SIMULIA ABAQUS, the preferred damage initiation criteria for fiber-reinforced composites are based on the previously stated Hashin's theory. Using the ply strength properties of the material, ABAQUS is able evaluate and determine the damage initiation, from the equation $\sigma = \mathbf{M}\hat{\sigma}$, where σ is the true stress, and $\mathbf{M}$ is the damage operator:

$$\mathbf{M} = \begin{bmatrix} \frac{1}{1-d_f} & 0 & 0 \\ 0 & \frac{1}{1-d_m} & 0 \\ 0 & 0 & \frac{1}{1-d_s} \end{bmatrix} \tag{3.5}$$

where d_f, d_m and d_s are internal damage variables that characterize fiber, matrix, and shear damage. They are derived from damage variables ${d_f}^t, {d_f}^c, {d_m}^t$ and ${d_m}^c$ corresponding to the four damage initiation mechanisms previously discussed, as follows [26]:

$$\begin{aligned} d_f &= \begin{cases} {d_f}^t \text{ if } \hat{\sigma}_{11} \geq 0 \\ {d_f}^c \text{ if } \hat{\sigma}_{11} < 0 \end{cases} \\ d_m &= \begin{cases} {d_m}^t \text{ if } \hat{\sigma}_{22} \geq 0 \\ {d_m}^c \text{ if } \hat{\sigma}_{22} < 0 \end{cases} \\ d_s &= 1 - (1 - {d_f}^t)(1 - {d_f}^c)(1 - {d_m}^t)(1 - {d_m}^c) \end{aligned} \tag{3.6}$$

During the elastic behavior, before damage initiation, $\mathbf{M}$ is equal to the identity matrix, so $\hat{\sigma} = \sigma$. Once damage initiation has occurred for at least one mode, $\mathbf{M}$ becomes significant in the criteria for damage initiation of other modes. The effective stress $\hat{\sigma}$, represents the stress acting over the damaged area that effectively resists the internal forces.

To work with $\hat{\sigma}$, ABAQUS introduces a characteristic length into the formulation, which allows to relate stress-displacement. Each of the damage variable will evolve with a stress-displacement behavior as shown in Figure 3.1. The positive-slope part of the triangle corresponds to the typical linear elastic material behavior, prior to damage initiation

[26]. When the highest point of the triangle is reached, damage begins and that damage criterion has met its critical value. With the available material properties, ABAQUS is not able to model the negative slope of the triangle, which would correspond to the damage propagation. The fracture energy is defined by the area under the positive-slope side of the triangle.

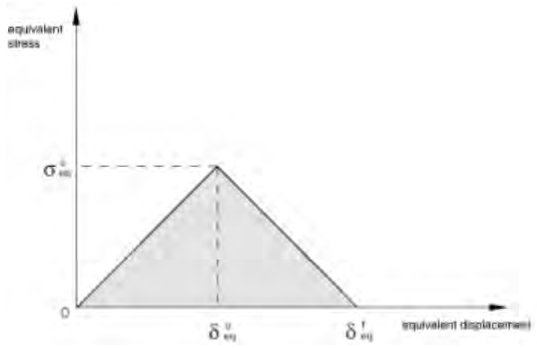

Figure 3.1: Equivalent stress vs. equivalent displacement [26]

ABAQUS also allows the user to choose between the model presented by Hashin and Rotem, by choosing $\alpha = 0$ or the one proposed by Hashin setting $\alpha = 1$ [26]. There are four output variables, one for each of the damage initiation mechanisms, indicating whether the specific criterion has been met. A value of 1 or higher is given if satisfied.

4. NUMERICAL MODELS

In this section it is explained thoroughly step by step the definition of the different FEM models that will be implemented in ABAQUS software in order to simulate the experimental procedures carried out by the different authors this thesis is interested in, by means the definition of geometries, material properties and boundary conditions, the models are to be accurate representations of the reality.

4.1. Finite Element Method

4.1.1. General definition

Finite Element Method, normally stated as FEM, is a numerical method used mainly in mathematical and engineering fields to solve complex, continuous problems in which analytical solutions cannot be achieved. The key of this numerical method is that it divides the original large problem into smaller and simpler parts where differential equations can be solved. Originated in the 1940s as a necessity to solve the complicated problems related to elasticity and structural analysis found in aerospace engineering, FEM has allowed the scientific community to perform experiments and test prototypes along these years, with a substantial reduction in both economic and time costs.

Finite Element Method works the following way: starting with the continuous problem along with the complex set of differential equations that defines it, FEM firstly subdivides this complicated domain into several, smaller regions, simple enough for the differential equations to be approximately solvable. This process is known as discretization. Each one of this regions is referred as an 'element'. The different elements are interconnected at specific points, called 'nodes'. On each of these elements, the original, complex set of equations are applied, which means that for N elements, there are N sets of equations. It is in the nodes where the discrete solutions for different variables (such as displacement in a given direction) are determined. The degree of freedom of a node is given by the number of unknown variables found at it. A system of linear algebraic equations results from assembling the element equations for each region, which can be

easily solved by a computer if put in matrix form [16].

Although there are several commercial software that implement the Finite Element Method to solve engineering problems, all of them have the following essential components:

- *Preprocessor*: the real problem is modeled by means of geometry, material properties and boundary conditions. Mesh refinement is also needed in order to set accurate the solutions are desired to be.
- *Solver*: the set of equations are solved for each region and node, by means of FEM.
- *Postprocessor*: results are shown to the user by graphical means, such as plots and fields. It also allows for further analysis of the resultant data.

4.1.2. FEM and composite materials

Being an expensive material to manufacture, composites designers had to find a way to build and test its prototypes, without having to actually produce them in real life. The solution to this problem was found in Finite Element Method. FEM software allows a cost-efficient, almost infinite way of testing. Needing only sufficient computational capabilities, composites can be accurately simulated, saving all the costs that physical tests would mean.

For this thesis, SIMULIA ABAQUS is used. Developed by Dassault Systèmes, ABAQUS is a powerful calculation tool used in engineering industry. Thanks to its FEM implementation, ABAQUS is able to solve complex problems, such as structural analysis. Using its postprocessor capabilities, a wide range of result analysis can be carried out depending on the user's desired tasks.

4.2. Geometry

The first step needed to implement a model of a real specimen, is to determine its geometrical dimensions. This initial section is devoted to dimensionalizing the specimens used in the real experiments in ABAQUS, as well as implementing the composite layup using the available tools in the software.

4.2.1. Pinho's research

The experiments that are to be modeled are known as 'Compact Tension/Compression Tests'. Developed by the American Society for Testing and Materials (ASTM), these standard tests are use for the determination of the fracture toughness of the different materials. Although originally developed for metals, with some slight modifications they can also be used to perform different analysis on composite materials. In order to hold the specimen to be tested, a clevis and pin arrangement is used. A controlled load is applied on the pre-cracked sample, while the displacement-load data is recorded. With a post-analysis of the experimental data, the fracture toughness of the material can be obtained in terms, for example, of the J-integral.

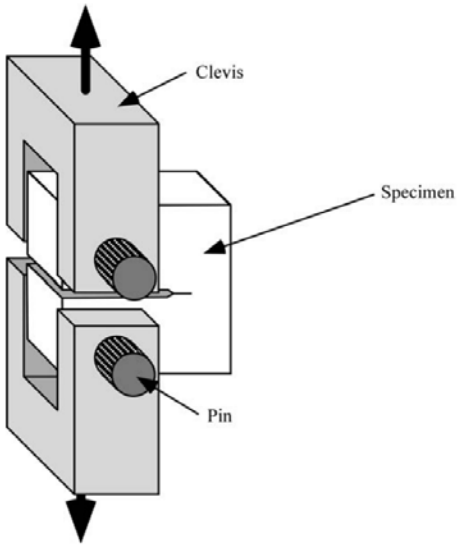

Figure 4.1: Apparatus for testing compact specimens [25]

The test specimens used by Pinho in his research [12] are the following:

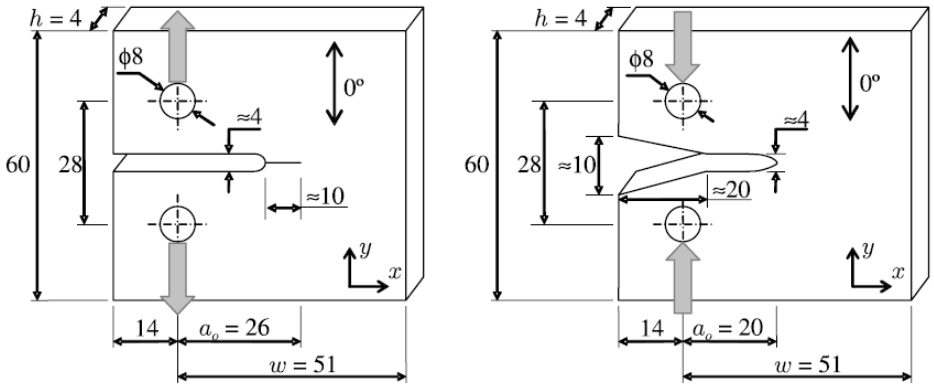

Figure 4.2: Dimensions (mm) for Tensile (left) and Compression (right) tests [12]

It can be clearly seen that both geometries have a symmetry along their horizontal axis. This symmetry will be taken advantage of in ABAQUS. If only half the geometry has to be modeled, everything related to computational time costs can be divided by two. ABAQUS will be later in charge of automatically adjusting the results obtained in the solver in order to obtain the appropriate data. In Figure 4.3, the geometry in ABAQUS of half a specimen for the compact tension test is shown. It can be seen that the notch is different compared to that found in Pinho specimens. It was modeled this way for a better mesh refinement, and as shown by Jackson and Ratcliffe [15], the results are not significantly affected by the morphology of the notch opening. The same can be appreciated for the compact compression specimen in Figure 4.4, in which the notch opening is widened to avoid contact of the faces during the test.

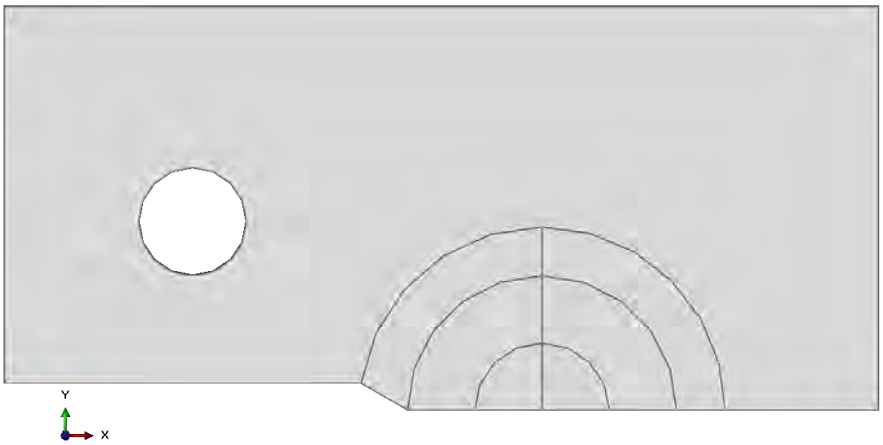

Figure 4.3: Modeled specimen for CT test

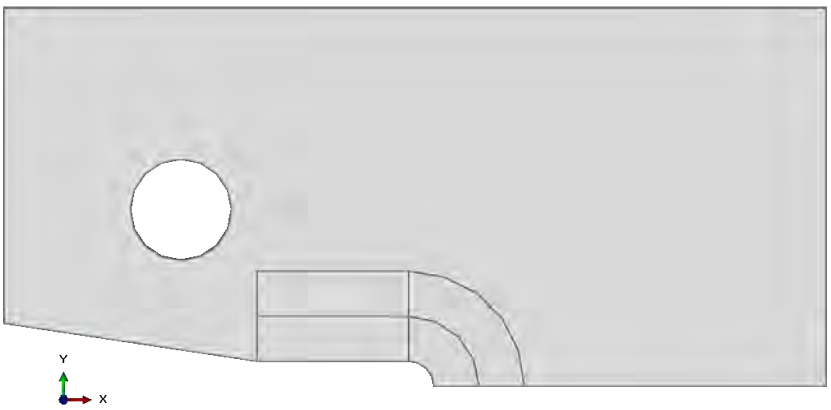

Figure 4.4: Modeled specimen for CC test

4.2.2. Catalanotti's research

Catalanotti's goal with his research [13] is to determine the compressive crack resistance curve of some composites. In order to do so, the geometry of the specimens and the experimental procedure is different to that of Pinho. Catalanotti performs different tests in double-edge notched specimens, by applying a controlled displacement and measuring the load.

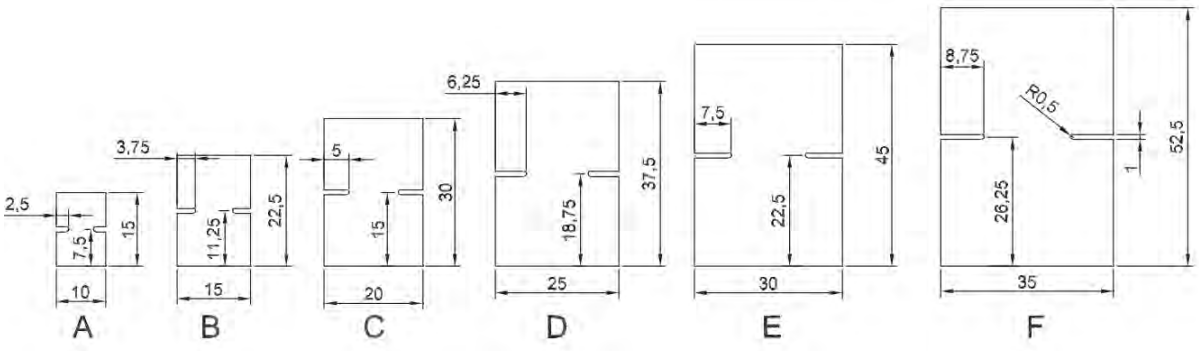

Figure 4.5: Specimens dimensions (mm) [13]

Symmetry can also be applied to the implemented models of the test specimens. Thanks to it, only a quarter of the specimen needs to be modeled, reducing significantly the computational cost.

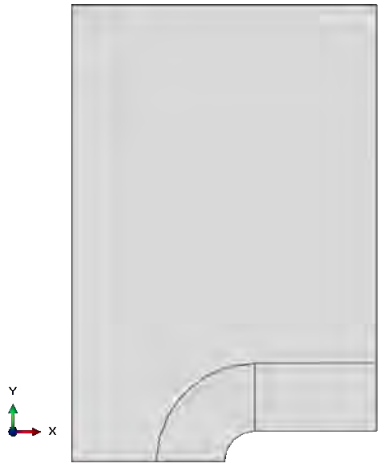

Figure 4.6: Modeled A-specimen for Catalanotti's simulation

4.2.3. Composite layup

Within *Property* tab, ABAQUS offers the possibility to accurately simulate a composite layup. The input parameters the software needs are the number of desired plies, the regions in which the layup will be applied, as well as the material, thickness and rotation of each ply. For modeling Pinho's specimens as an example, which have a layup $(90, 0)_{8S}$, 16 plies of 0.125mm thickness each will be implemented in ABAQUS, applying the material properties previously defined. The 'symmetry option' will be enabled in order to easily conform the total 32 layers of the real, 4mm-thick specimen.

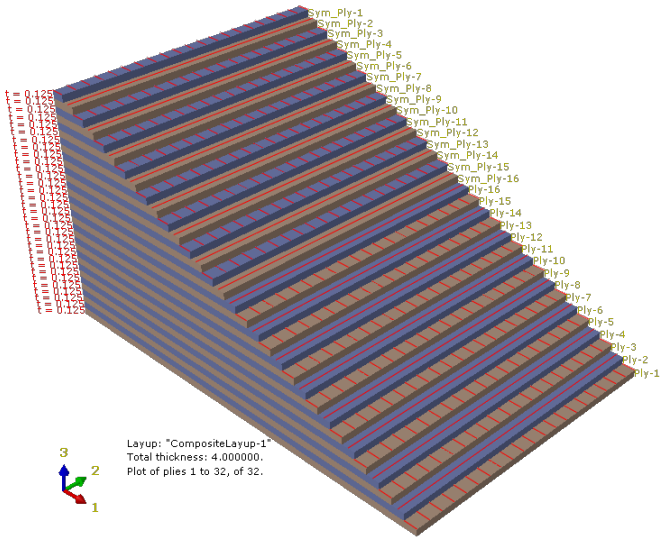

Figure 4.7: Modeled composite layup for one of Pinho's test specimens

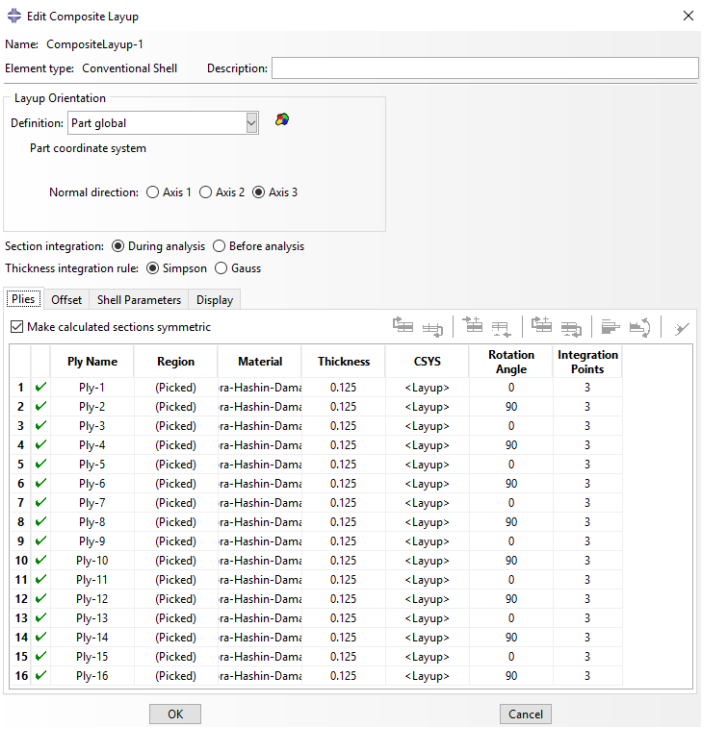

		Ply Name	Region	Material	Thickness	CSYS	Rotation Angle	Integration Points
1	✔	Ply-1	(Picked)	ra-Hashin-Dama	0.125	<Layup>	0	3
2	✔	Ply-2	(Picked)	ra-Hashin-Dama	0.125	<Layup>	90	3
3	✔	Ply-3	(Picked)	ra-Hashin-Dama	0.125	<Layup>	0	3
4	✔	Ply-4	(Picked)	ra-Hashin-Dama	0.125	<Layup>	90	3
5	✔	Ply-5	(Picked)	ra-Hashin-Dama	0.125	<Layup>	0	3
6	✔	Ply-6	(Picked)	ra-Hashin-Dama	0.125	<Layup>	90	3
7	✔	Ply-7	(Picked)	ra-Hashin-Dama	0.125	<Layup>	0	3
8	✔	Ply-8	(Picked)	ra-Hashin-Dama	0.125	<Layup>	90	3
9	✔	Ply-9	(Picked)	ra-Hashin-Dama	0.125	<Layup>	0	3
10	✔	Ply-10	(Picked)	ra-Hashin-Dama	0.125	<Layup>	90	3
11	✔	Ply-11	(Picked)	ra-Hashin-Dama	0.125	<Layup>	0	3
12	✔	Ply-12	(Picked)	ra-Hashin-Dama	0.125	<Layup>	90	3
13	✔	Ply-13	(Picked)	ra-Hashin-Dama	0.125	<Layup>	0	3
14	✔	Ply-14	(Picked)	ra-Hashin-Dama	0.125	<Layup>	90	3
15	✔	Ply-15	(Picked)	ra-Hashin-Dama	0.125	<Layup>	0	3
16	✔	Ply-16	(Picked)	ra-Hashin-Dama	0.125	<Layup>	90	3

Figure 4.8: Composite Layup editor available in ABAQUS

4.3. Material

The definition of reliable properties of the materials is a key relevant factor when performing a FEM analysis. ABAQUS a great variety of material characteristics to be defined, depending on the material to be simulated. Composites are strongly anisotropic materials, where its behavior changes according to the direction of the applied loads. For this reason, they will be simulated in ABAQUS as laminae. Firstly, perfectly elastic properties are introduced in ABAQUS, in order to model the first steps prior to damage initiation. Values for $E_1, E_2, G_{12}, G_{23}, G_{13}$ and ν are defined in this step. As the way damage initiates is of interest for this thesis, a damage model is to be implemented. ABAQUS offers for fiber-reinforced composites a model based on Hashin's theory, both 1973 and 1980 versions. In order to do so, ABAQUS needs both longitudinal and transverse, tensile, compressive and shear strengths to be specified.

It is important to remark that, for unidirectional fiber-reinforced composites, in order to obtain a trustworthy set of properties, a thorough study needs to be carried out, involving many test methods, both standard and non-standard ones. The fact that every direction of the material (longitudinal, transverse and shear) is to be analyzed, and the differentia-

tion needed for tension and compression, as this will sufficiently affect the results, makes acquiring a reliable data even more tedious.

Because of this, not all properties needed by ABAQUS to perform the simulations could be found in the literature, due to that in some cases, they simply have not been studied. Some assumptions are then taken, based on similar composites materials, in order to fulfill these requirements. This procedure can be understood with the following:

Taking the mechanical properties of the materials used by Pinho [12] and Catalanotti [13], specified in their respective papers:

E_1 *(GPa)*	E_2 *(GPa)*	G_{12} *(GPa)*	ν_{12} *(-)*
131.7	8.8	4.6	0.32

TABLE 4.1. PINHO'S T300/913 PROPERTIES

E_1 *(GPa)*	E_2 *(GPa)*	G_{12} *(GPa)*	ν_{12} *(-)*
171.42	9.08	5.29	0.32

TABLE 4.2. CATALANOTTI'S IM7-8552 PROPERTIES

It is easily seen that some important properties, like shear modulus G_{13} and all Hashin's strength properties, are missing. The solution found in order to be able to perform the simulations in ABAQUS was to use the material properties of a similar unidirectional composite, *AS4-8552*, that was studied in detail by Falcó et al. [14].

Elastic properties		*Strength properties*	
E_{1t} (GPa)	137.1	X^T (MPa)	2106.4
E_{1c} (GPa)	114.3	X^C (MPa)	1675.9
E_{2t} (GPa)	8.8	Y^T (MPa)	74.2
E_{2c} (GPa)	10.1	Y^C (MPa)	322.0
$G_{12} = G_{13}$ (GPa)	4.9	S^L (MPa)	110.4
$\nu_{12} = \nu_{23}$ (-)	0.314	S^T (MPa)	110.4

TABLE 4.3. AS4-8552 PROPERTIES

4.4. Boundary conditions

The definition of the proper boundary conditions is important to accurately implement in the model the conditions applied to the real specimen. As symmetry is being used to reduce the computational cost, first of all must these conditions be applied to the model. In Pinho's case, only y-symmetry must be defined, while Catalanotti's modeled specimens need both x- and y-symmetries to be properly applied. Thanks to this, ABAQUS is now able to identify the not-defined portions of the real model in order to carry out the complete calculations.

Both researchers rely on controlled displacements to perform their experiments. Using the adequate instruments, one can know the reaction force exerted by the studied piece for each displacement increment. This can be applied in ABAQUS in several ways. The one used in this thesis is applying a known displacement in a surface (Catalanotti) or to a pin (Pinho). For the pin case, a interaction must be defined between the modeled pin and the surface it is 'contact' with, in order to properly simulate the situation faced in reality.

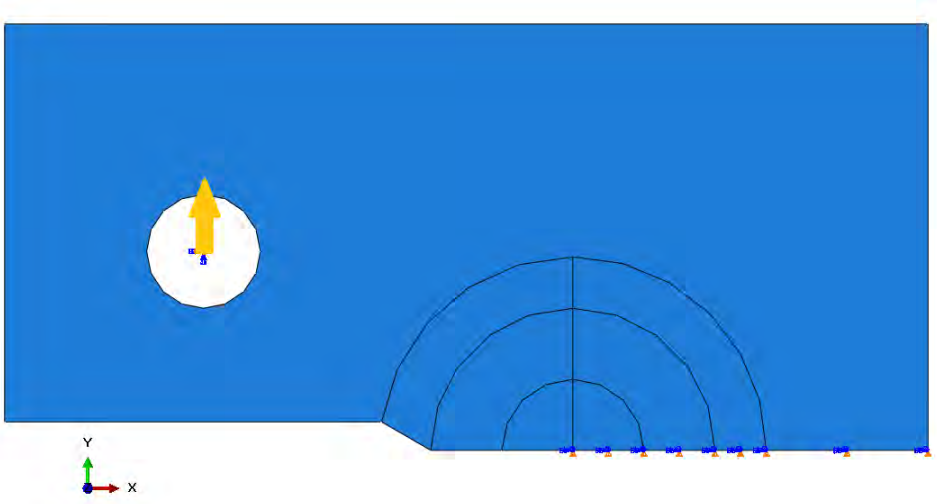

Figure 4.9: Boundary conditions applied to modeled CT Pinho's specimens. Pin displacement (orange arrow) and y-symmetry can be appreciated

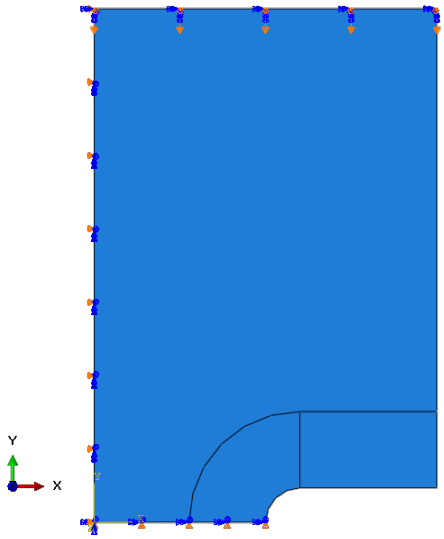

Figure 4.10: Boundary conditions applied to modeled Catalanotti's specimens. Surface displacement and x-,y-symmetries can be appreciated

4.5. Crack definition

Related to Fracture Mechanics, there are different options available in ABAQUS that can be used to study this interesting topic. virtual crack closure technique (VCCT) and extended finite element method (XFEM) allows the user to study the initiation and propagation of cracks along surfaces. Unfortunately, they are not accessible in the ABAQUS version used for this thesis (ABAQUS/Implicit). On the other hand, contour integrals are available to study the initiation of cracking quasi-static problems, which are the case of interest.

The procedure to be followed starts with the definition of the crack front, which is the forward part of the crack. This first step is important, as ABAQUS will use this feature to calculate the first contour integral, by means of the elements included in it and the first layer of elements outside the front. Different entities can be selected as the crack front, including a single vertex (like for Pinho's CT models) or an edge (such as Pinho's CC and Catalanotti's models).

Next step includes the definition of the crack tip. For 2D parts like the ones in this thesis, this must be a single node or vertex. It is in this selected element where the crack extension direction q will be specified. It has to be pointing into the material, parallel to the crack, in order to obtain positive J-integral values.

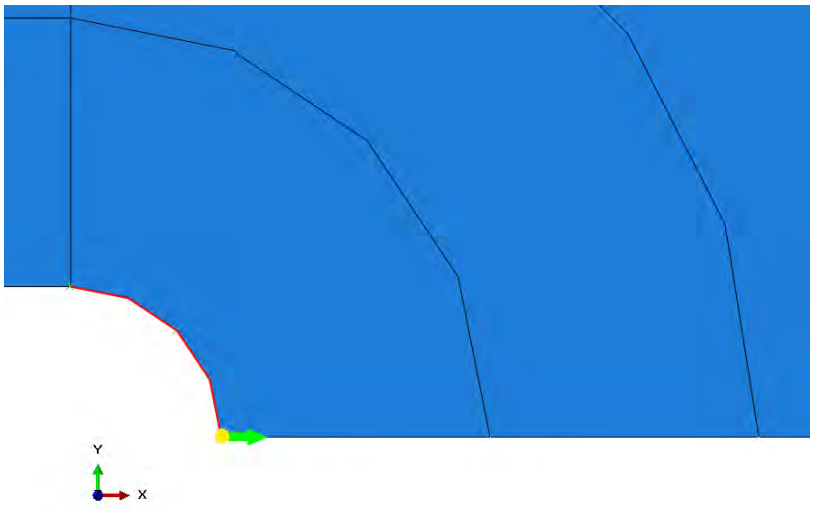

Figure 4.11: Crack in a CC specimen. Crack front (red), tip (yellow), q vector (green)

A refined mesh is needed around the crack tip, as large stresses concentrates at this location, so accurate results can be then achieved. For CT specimens, where the geometry of the region supposes a sharp crack, the results around the tip may become singular. This can be controlled in ABAQUS by specifying some parameters: for an elastic materials (as composites are defined in this thesis), a $1/\sqrt{r}$ singularity is to be used. ABAQUS will then mode the mid-side nodes to the $1/4$ points, in order to improve the accuracy of the contour integral calculations.

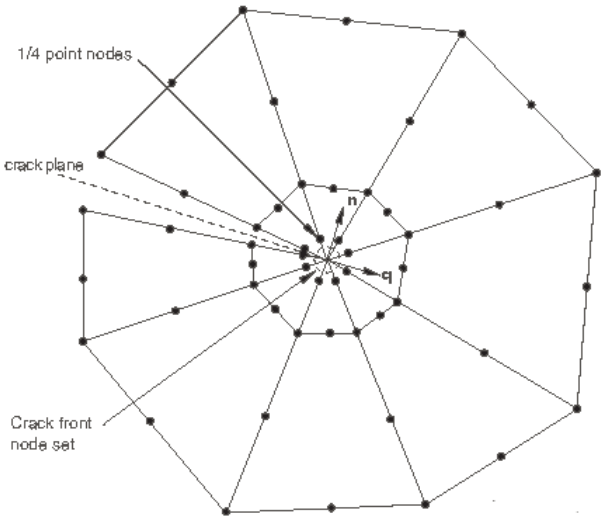

Figure 4.12: Typical mesh for crack evaluation with 1/4 point nodes [26]

4.6. Step definition

It is in the *Step* module of ABAQUS where some of the most relevant parameters of a model have to be defined. The user can define which type of analysis they want to perform, using the Step manager. By defining the incrementation details, it is possible to specify the precision with which ABAQUS collects the results of the equations is told to solve using the Finite Element Method. A low time-step size means that data is gathered more frequently leading to more precise results. Especially in ABAQUS/Implicit, the software version used for this thesis, 'time' variable does not really have a 'physical' meaning, and it is only used to determine for example, what percentage of a load is applied for that step. Applying this to this thesis, the 1-mm displacement within a 1-s time definition used for Pinho's models, means that 100% (1 mm) of the specified displacement has been applied by the end of the procedure.

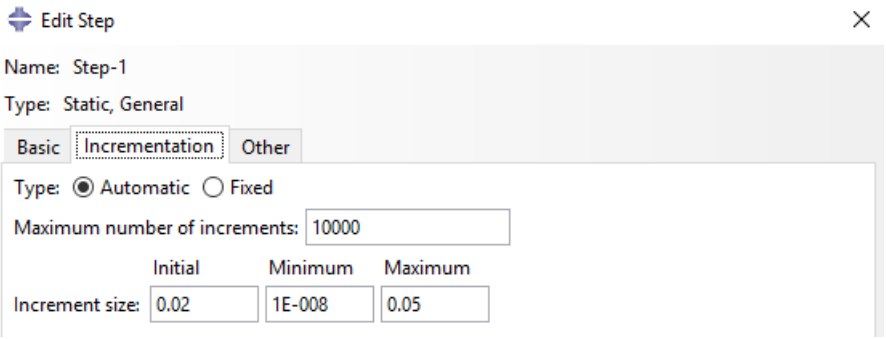

Figure 4.13: Incrementation details used for an accurate result collection

Step module is also used to specify which variables must ABAQUS write in the output file. The ones interesting for the development of this thesis are those related to damage criteria (Hashin's damage variables), energy release rates, as well as reaction forces and translations in the points of load application.

4.7. Mesh

The mesh refinement is one of the most important aspects of a FEM model, at the same level as geometrical dimensions. The results are greatly influenced by the mesh definition, something that can be easily seen if one pays attention to the basics of how Finite Element Method works. Having a poor quality, or incorrectly defined mesh will lead to a significant inaccuracy of the results, yielding for example impossibly large numbers for an applied force. Because of this importance, the ideal solution would be to a mesh so much refined, that it has almost an infinite numbers of elements. The highest accuracy of the results would be achieved, and it would be a perfect model of the reality. But it cannot be actually done this way: a mesh this refined would mean an enormous calculation time, being highly cost-inefficient. This is why a sensible mesh refinement is needed, in order to achieve sufficiently accurate results, while at the same time keeping computational costs within a logical margin.

ABAQUS offers different tools to do so. One of the simplest available is using partitions. As it could be seen in figures of modeled specimens in Section 4.2, the geometry of the modeled specimen has been partitioned by means of circular lines centered on the crack tip. Thanks to this strategy, a focused mesh can be better generated around the crack, which is the area of interest for obtaining the desired data. When applying the meshing conditions, these circular areas are heavily meshed using 'swept' technique, which yields a regular and focused mesh, as ABAQUS generates a ring of collapsed, quadratic elements, as it can be seen in Figure 4.15. It is important that a sufficient number of elements is generated around the crack in order to obtain accurate results, as they are very sensitive to the mesh refinement. The other areas of the model are free-meshed, using the 'medial axis' technique. The number of elements in these areas is fewer, as they will not play such an important role in the accuracy of the determination of the final results, yielding a less-demanding computational cost.

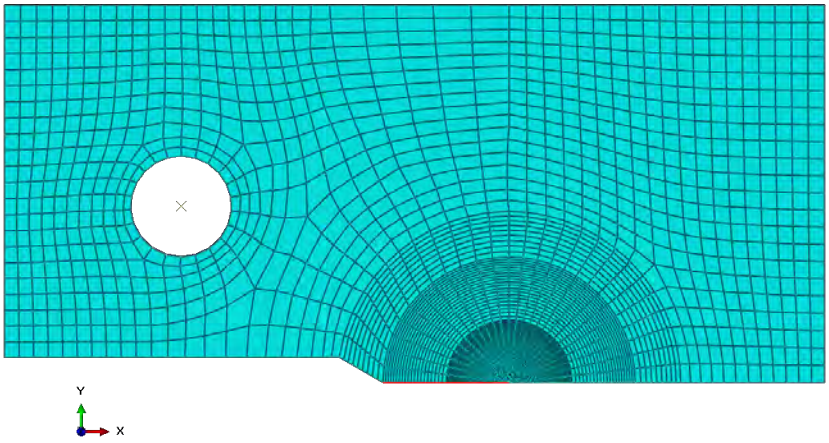

Figure 4.14: Mesh refinement for Pinho's CT specimen (crack location highlighted in red)

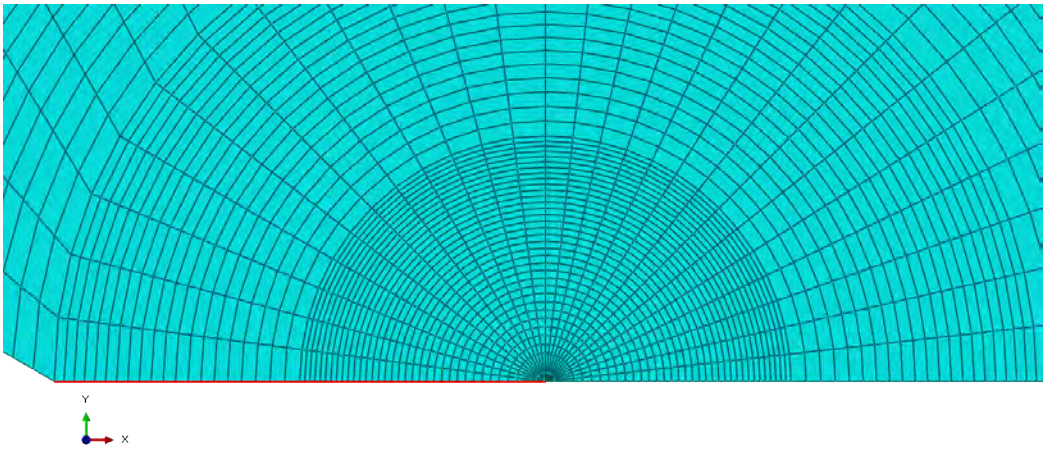

Figure 4.15: Closeup on the crack tip. Dense, swept element area can be appreciated

5. RESULTS AND DISCUSSION

In this section, the procedure used to validate the FEM implemented models is explained. A detailed analysis of the results is performed, stating the main drawn conclusions is included. At the end of the section, a parametric study and a comparison between the two methodologies is carried out.

5.1. Pinho's research

Pinho's goal with his research [12] is to experimentally measure the fracture toughness of a carbon-epoxy laminated composite, T300/913, associated to fiber tension and compressive fiber kinking, using compact tension and compression tests. By means of digital speckle photogrammetry and optical electron microscopy, he is able to determine the initiation and propagation values for critical energy release rates for both damage mechanisms.

This thesis is only interested in the initiation energy release rates: when the the composite specimen begins to fail due to damage initiation in its layup. The results obtained with the numerical models implemented in ABAQUS are to be compared with those obtained by Pinho in his study, which were a critical initiation energy release rates of $\mathbf{91.6\ KJ/m^2}$ and $\mathbf{79.9\ KJ/m^2}$ for tensile and compression tests, respectively. These values are the average that Pinho obtained for different pre-crack lengths.

In order to determine the energy release rates in the modeled specimens, Hashin's theory already implemented in ABAQUS was used. As stated in Section 4.3, the material characteristics for T300/913 composite stated by Pinho in his paper are missing the properties needed by Hashin's criteria. A composite material with similar mechanical properties was found and their strength characteristics summarized in Table 4.3 are assumed as valid for the composite of study.

The different steps needed by ABAQUS to properly carry out the FEM simulation were followed as stated in Section 4, along with a vertical displacement of 1mm applied to the pin. The results obtained are here analyzed. The implemented models were firstly

validated by means of the following procedure:

The J-integral energy release rate curves were obtained. Being modeled as a perfectly elastic material, the behavior of the curves shows a exponential grow as the displacement of the pin is increased, as it could be expected from the definition of the material type. Several contour integrals for the calculation of these energy rates were defined, being the first one preferably excluded, as suggested in the ABAQUS guide [26]. The results are seen to quickly converged, as all the contours starting already with the second one yield the same results. The value obtained by Pinho in his research [12] is now used, in order to establish the point in which the energy release rate of the simulated laminate would have change in shape, by means of a 'peak' in the visual representation, had the material properties been completely defined, as the real specimen does in the laboratory tests.

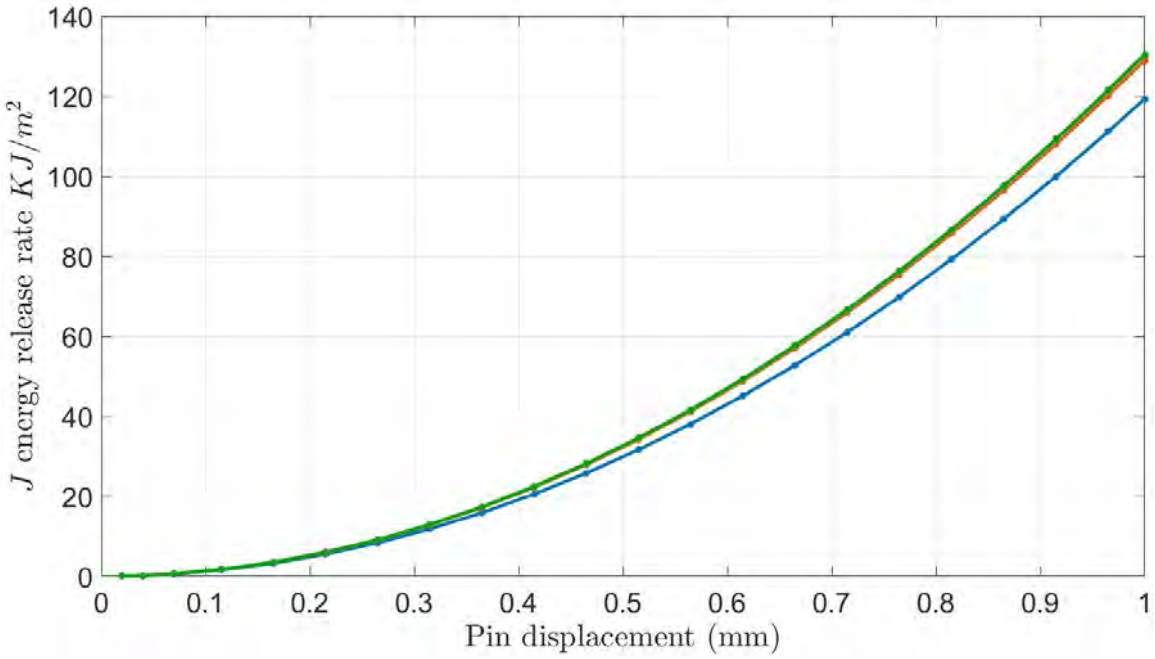

Figure 5.1: Energy release rate contours for $a_0 = 26mm$, CT specimen

This moment in time (as stated in Section 4.6, 'time' does not have a physical meaning in ABAQUS/Implicit) is used to analyze the different damage criteria developed in Hashin's theory.

Regarding the **Compact Tension** tests, the four Hashin's damage initiation mechanisms are plotted in Figures 5.2 and 5.3 differentiating 0^o and 90^o orientation layers, given a pre-crack length $a_0 = 26mm$. Each curve corresponds to one of the many elements the chosen mesh divides the modeled specimen in.

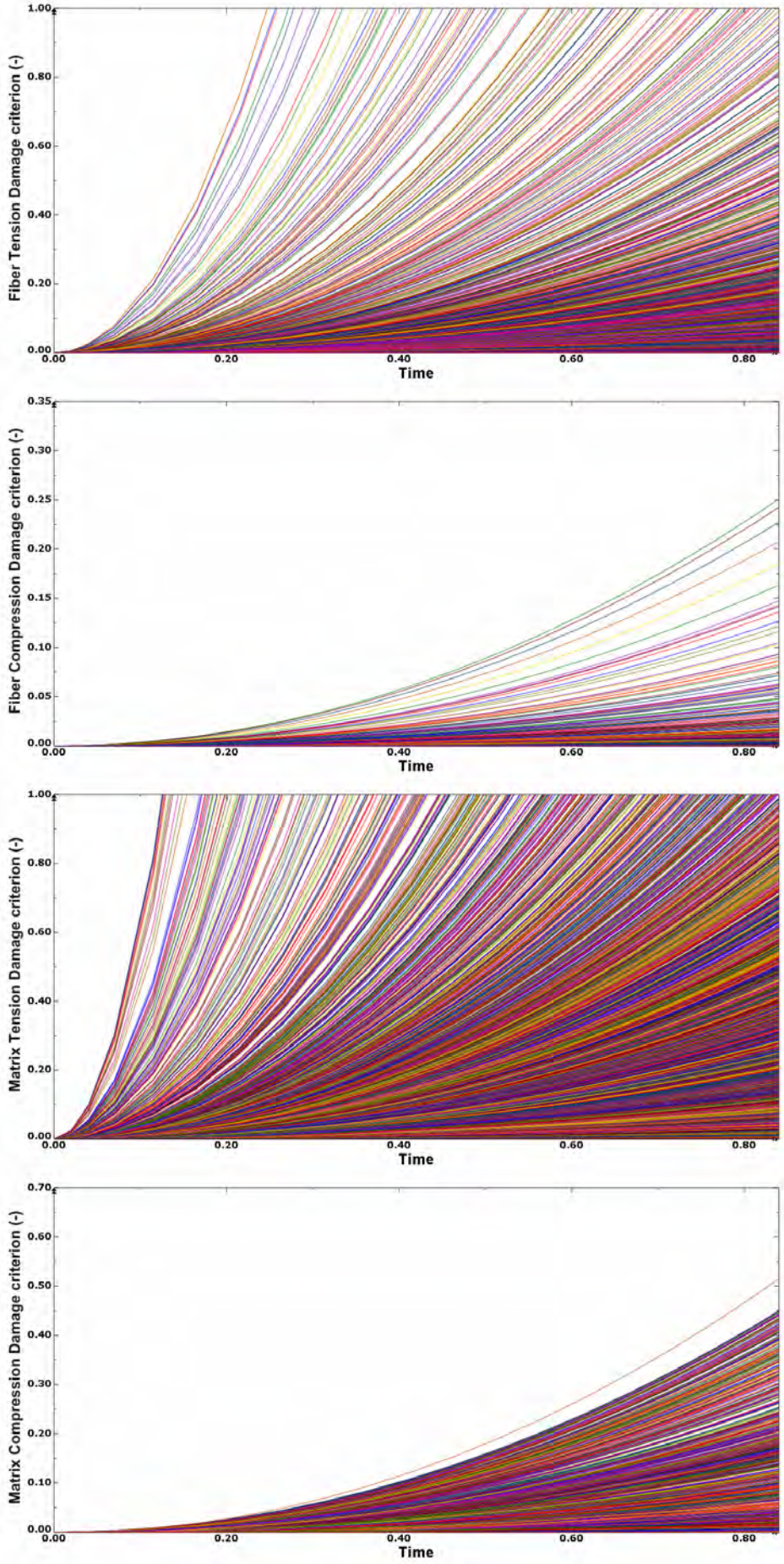

Figure 5.2: Hashin's damage mechanisms - CT, 0º layers

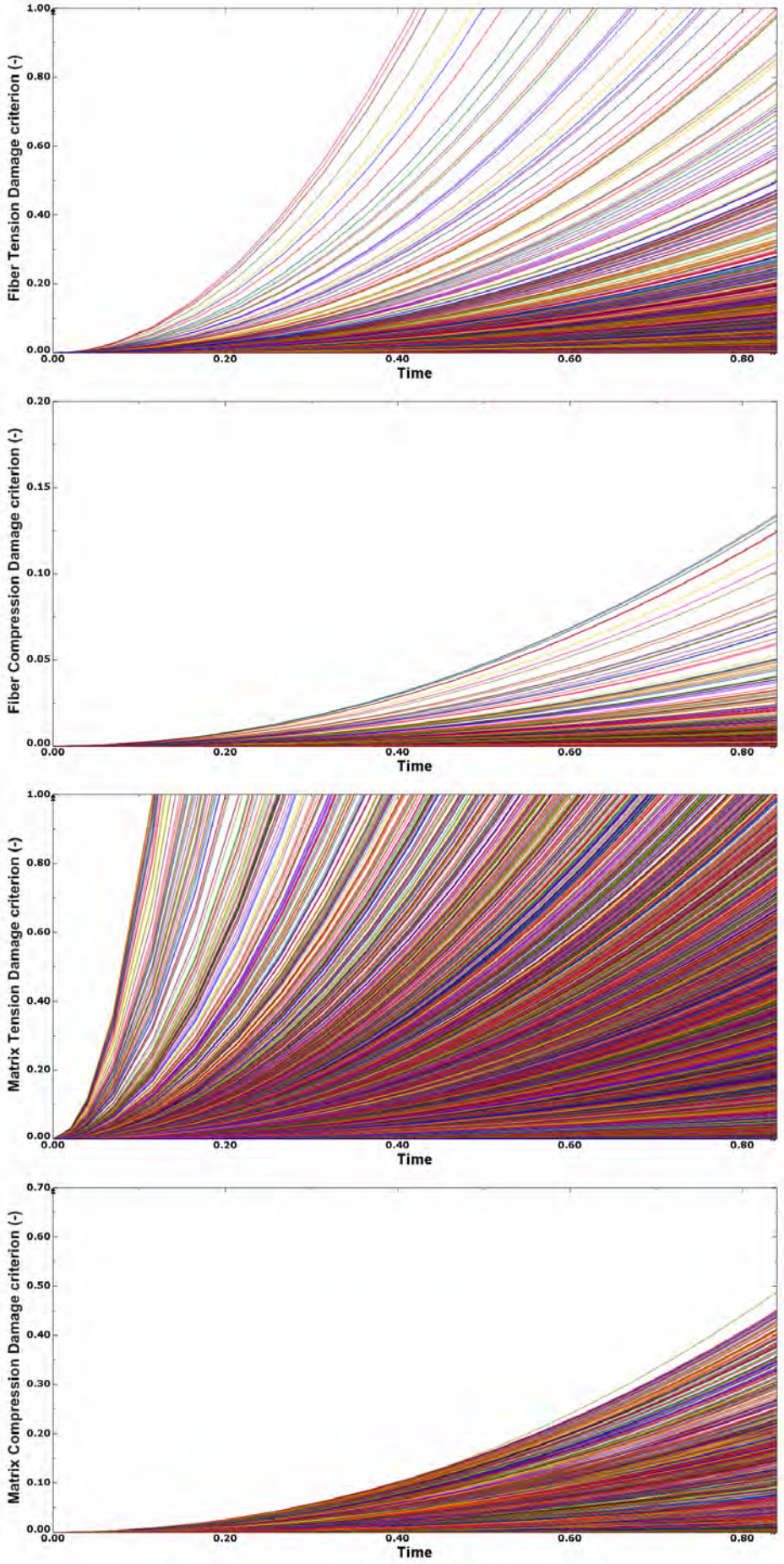

Figure 5.3: Hashin's damage mechanisms - CT, 90º layers

It can be seen that the weakest part of the laminates, the matrices, are heavily damaged under tension by the point the critical failure of the laminate is reached, as many elements are beyond the 'value equal to 1' threshold. This is as expected because the job of the matrix within the layer is not to carry the loads but to distribute them to the fibers and keep their orientation. The behavior of the matrix is very similar in both orientations.

Fiber Compression criterion values are analogous and it is not met for any of the orientations, as it could be thought beforehand, as it is a tension test the one being carried out.

It is *Fiber Tension* criterion the one of main interest. There are some differences in fiber performance in terms of the studied orientation of the layer. It can be seen that in the 0^o layers, those parallel to the loading direction, fibers start failing before the 90^o ones, as they reach the critical value sooner. One of the first conclusions that can be extracted from this fact is that, as it is known, Hashin's damage model is very conservative. A strict interpretation of his model would mean that once one of the four damage mechanisms is satisfied, the laminate as a whole is failing, and therefore, damaged. This conservative approach is intensified when applied to a FEM model, as the damage mechanisms can be studied for each element composing the model. It would not be sensible to state that, once a single element meets one of the damage mechanisms, the whole model is actually damaged.

The value for energy release rate obtained by Pinho [12] is assumed to be the critical one, in order to analyze the conservativeness of Hashin's damage model. The elements failing according to his damage criteria prior to the reach of Pinho's value are considered to be able to be withstood by the laminate, which will finally suffer ultimate failure and therefore, crack length would be propagated, at the moment the experimental value for energy release rate is achieved. The relationship between the number of failed elements according to Hashin's model and the pre-crack length a_0, different for each of the modeled specimens, can be then analyzed for further conclusions.

It is also interesting to graphically see the location of the failing elements when the crack propagation would initiate is the real specimen. Thanks to the tools offered by ABAQUS, contours like the ones shown in Figure 5.4 and 5.5 can be easily obtained (a deformation scale factor is applied). The elements plotted in color gray are the ones that

have already failed according to Hashin's *Fiber Tension* criterion. The difference between the two orientations can be also observed, as well as the heavy distortion suffered mainly by those elements close to the crack tip, which tells the user that important stresses have been experienced. The maximum values are reached at the very tip of the crack, as it could be expected, being the region with the highest stress and energy gradients.

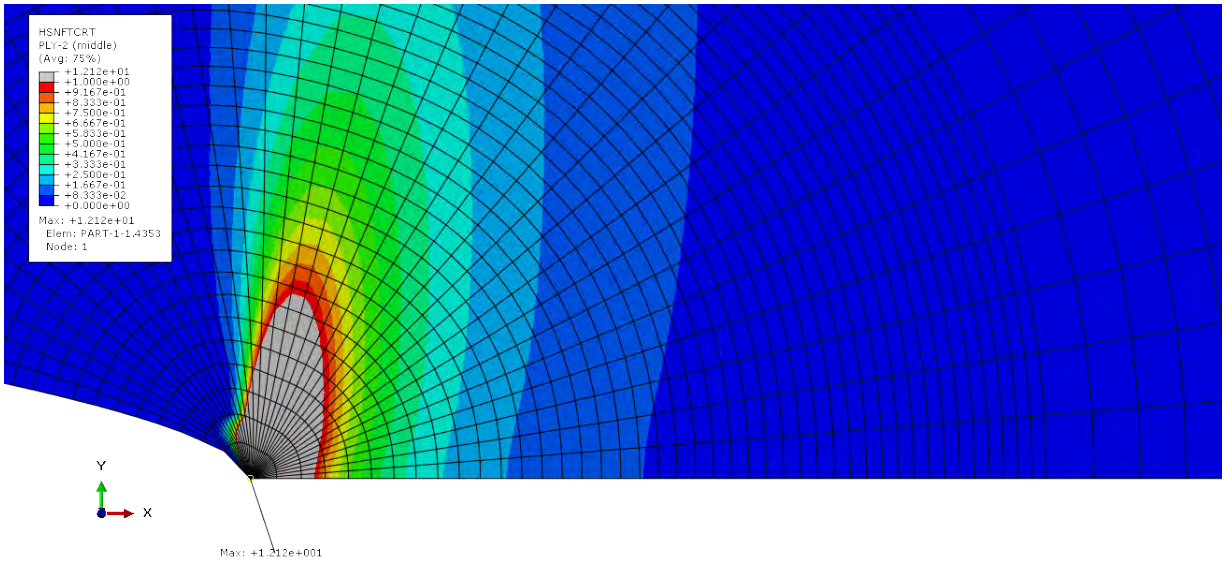

Figure 5.4: Hashin's FT criterion in 0º layer

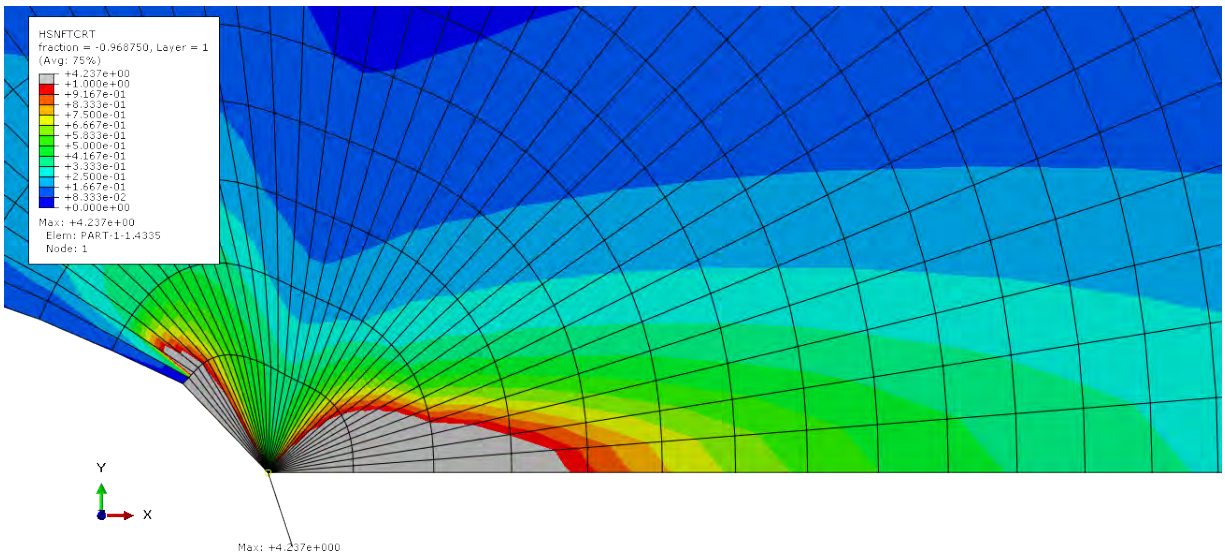

Figure 5.5: Hashin's FT criterion in 90º layer

Different specimens were modeled, according to the geometry dimensions specified by Pinho in his paper [12]. The pre-crack length a_0 was the only parameter changed along the specimens. Ranging from $a_0 = 24mm$ to $a_0 = 28mm$, the behavior of the laminate depending on this length was analyzed. The following table summarizes the results, which consists on the number of elements of the 90º layers that failed applying Hashin's FT damage mechanism prior to Pinho's energy release rate value, as a function of a_0:

Pre-crack length a_0 (mm)	*Failing elements according to Hashin*
24	21
25	23
26	25
27	27
28	26
Average no. of failing elements	**24.4**

TABLE 5.1. FT FAILING ELEMENTS AS A FUNCTION OF A_0 LENGTH

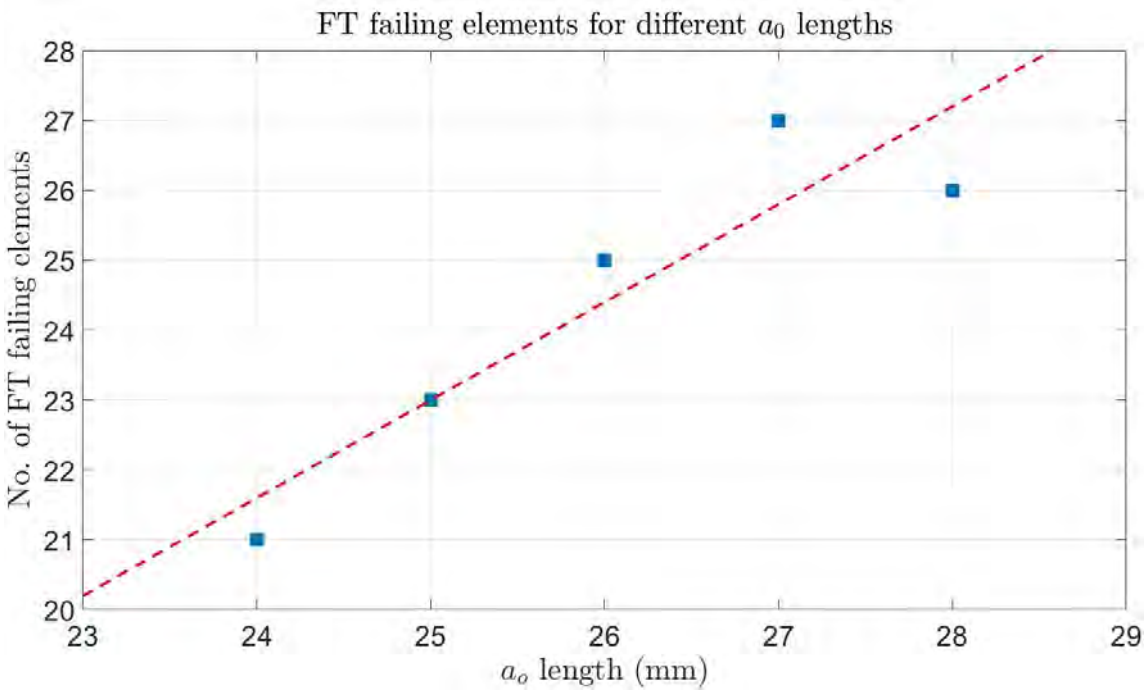

Figure 5.6: FT failing elements as a function of a_0 length

It can be easily observed in Figure 5.6 that the longer the pre-crack, the more elements are damaged according to Hashin's theory before the experimental value for energy release rate is reached. The explanation for this is that that the value Pinho states in his paper [12] is the average obtained for the different specimens, each with its respective a_0 value. If the individual J value had been provided, it can be confidently stated that the number of failing elements would had been constant, and not linearly increasing as in the existing models.

The J energy release rate is obviously also affected by the pre-crack length a_0. Choosing a contour integral in which the solution has already converged (practically any of them, except the first one), a comparison can be established in order to see the effect of a_0, as depicted in Figure 5.7. As it could be expected, larger values of a_0, corresponding to larger cracks, yield a gentler energy release rate curve. The simple reason behind this behavior can be stated as, the shorter the crack, the more material is to be damaged and therefore, the more energy is needed to do so.

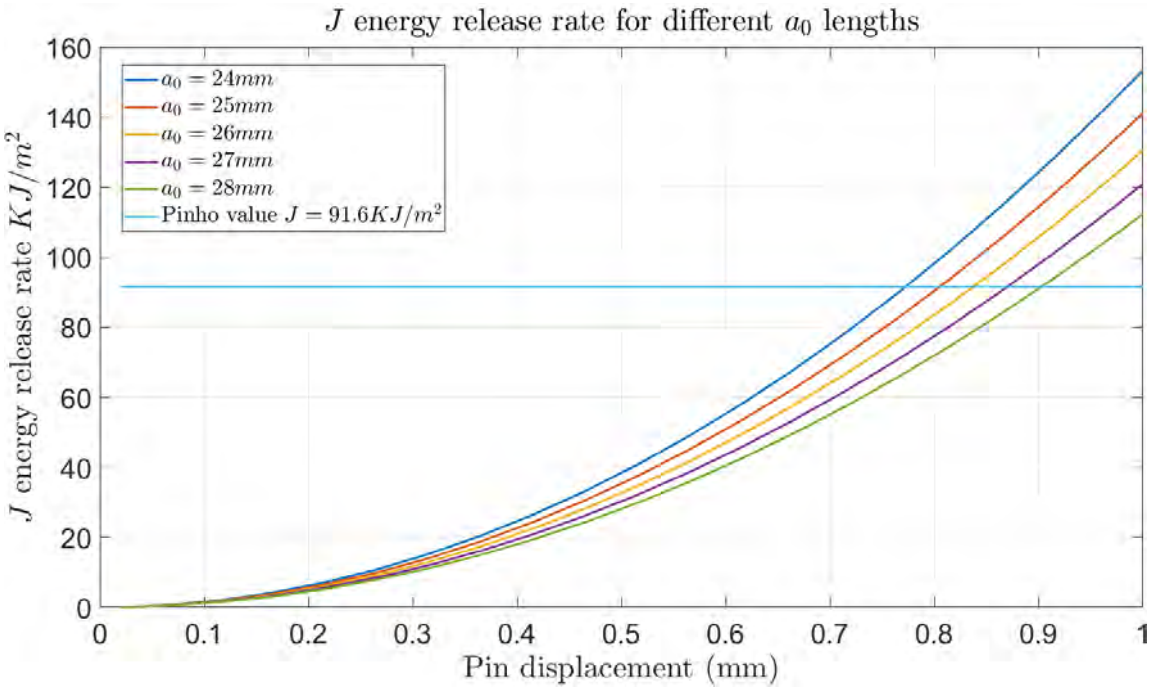

Figure 5.7: J energy release rates for different a_0 values

The **Compact Compression** modeled specimens were analyzed using the same procedure followed for the Compact Tension tests previously stated. The specimen with $a_0 = 20mm$ is taken as base case in order to explain the results in a more detailed way.

As it can be observed in Figure 5.8, all ten contours defined by ABAQUS to perform the J contour integrals converge and yield similar results. Any of them can be used for determining the moment of the simulation in which the experimental value for fracture energy was experimentally obtained by Pinho, which will be used for analyzing Hashin's damage criteria for the different orientations below.

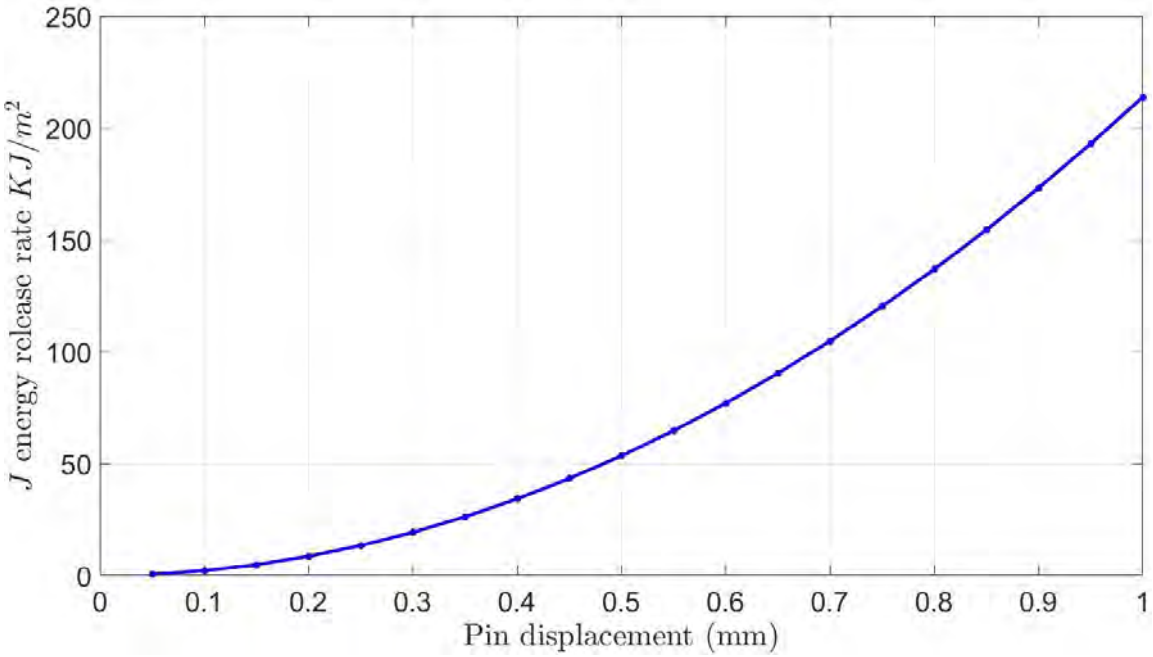

Figure 5.8: Energy release rate contours for $a_0 = 20mm$, CC specimen

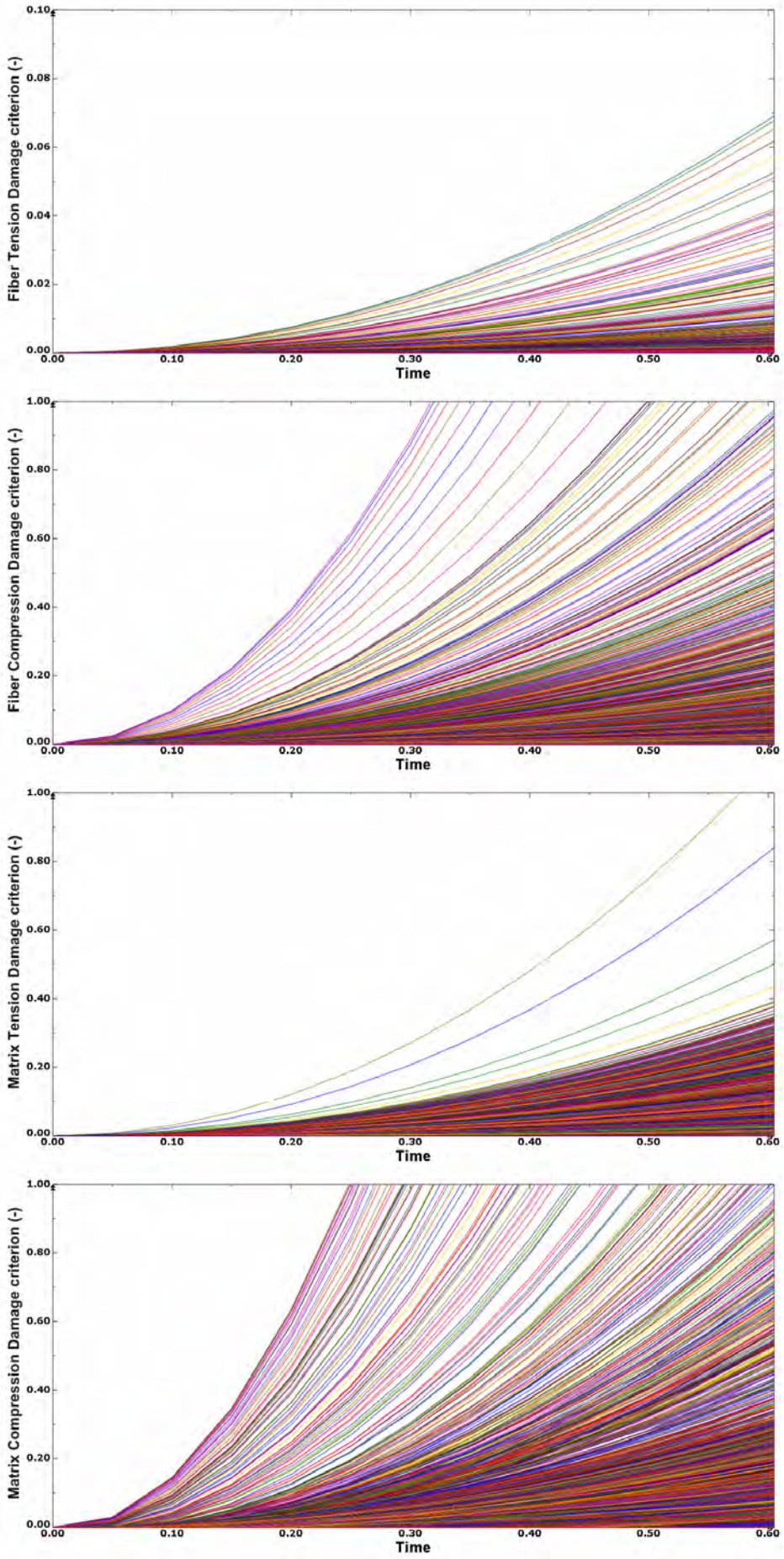

Figure 5.9: Hashin's damage mechanisms - CC, 0º layers

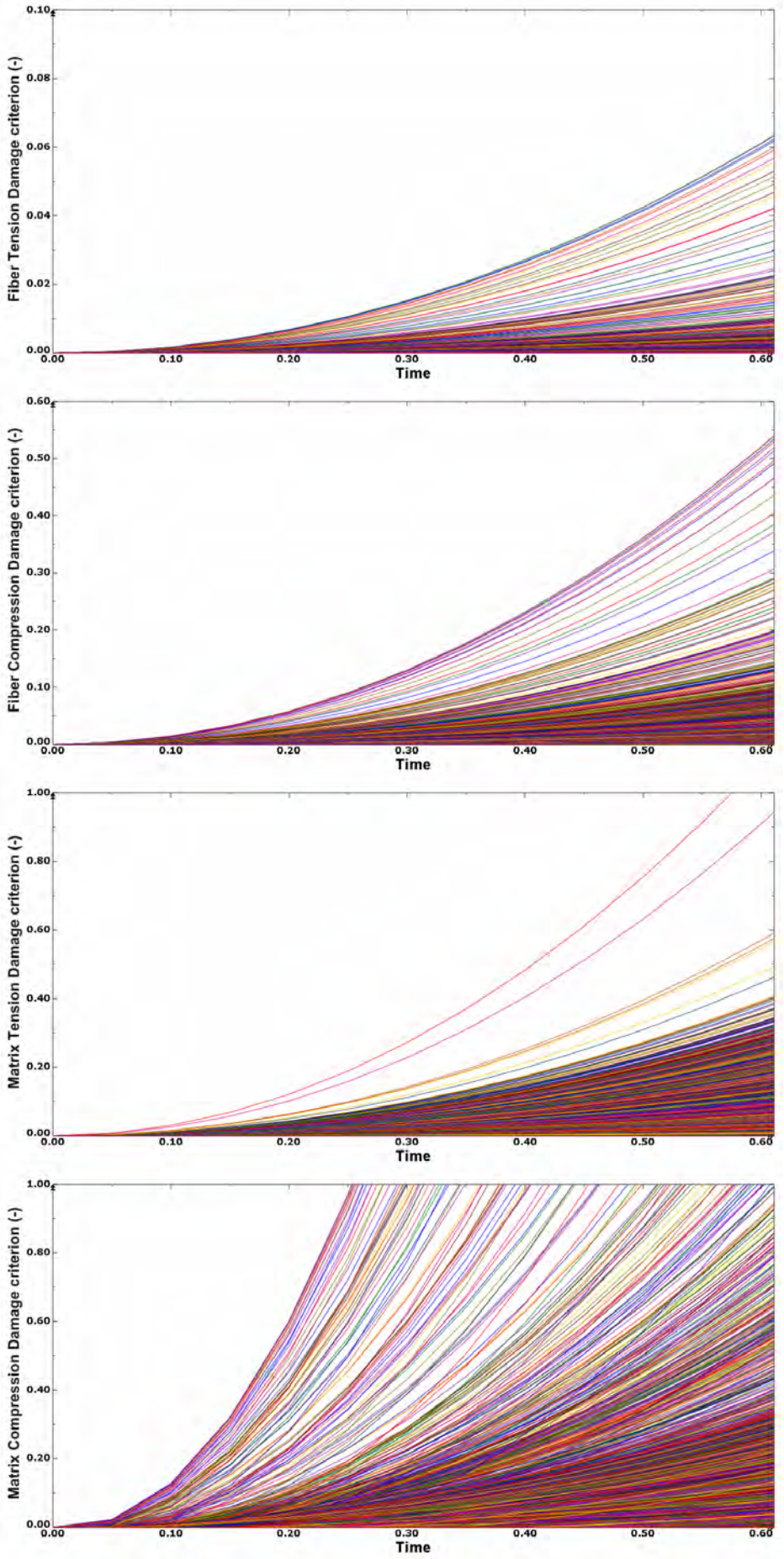

Figure 5.10: Hashin's damage mechanisms - CC, 90º layers

The data obtained regarding Hashin's damage mechanisms is plotted in Figures 5.9 and 5.10. As it was observed before, the two damage criteria corresponding to the other type loading application, i.e. tension for this case, are barely developed. Even that belonging to the matrix, the fragile component of the laminate, can be considered so as it is only one element, located at the surface in contact with the pin, which reaches a value equal to 1. The contours depicting the location of these failing elements are shown below, differentiating the layer orientation for better comparison.

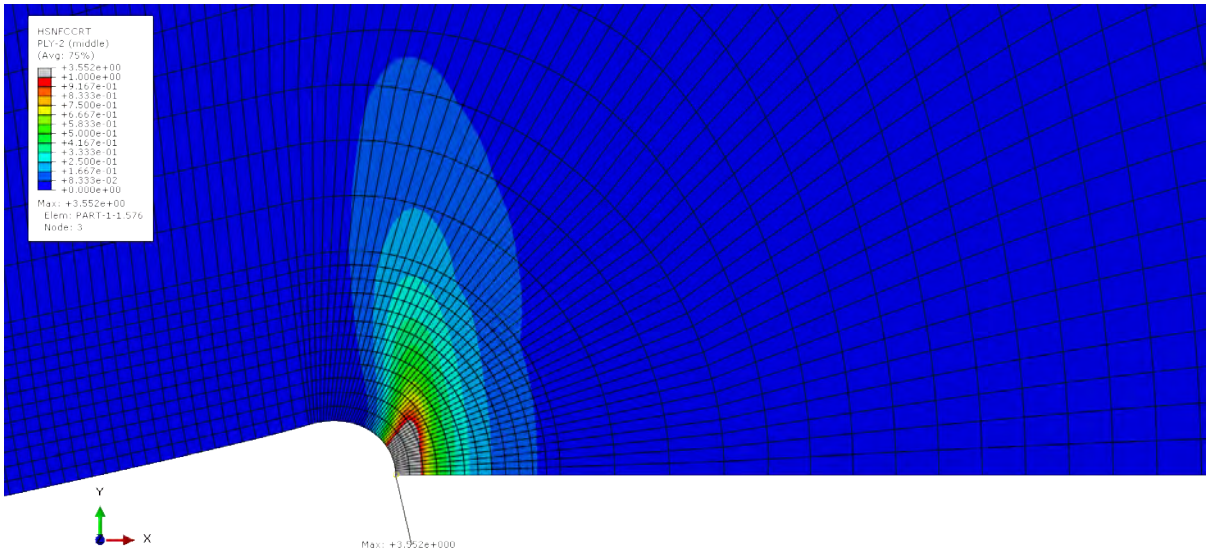

Figure 5.11: Hashin's FC criterion in 0º layer

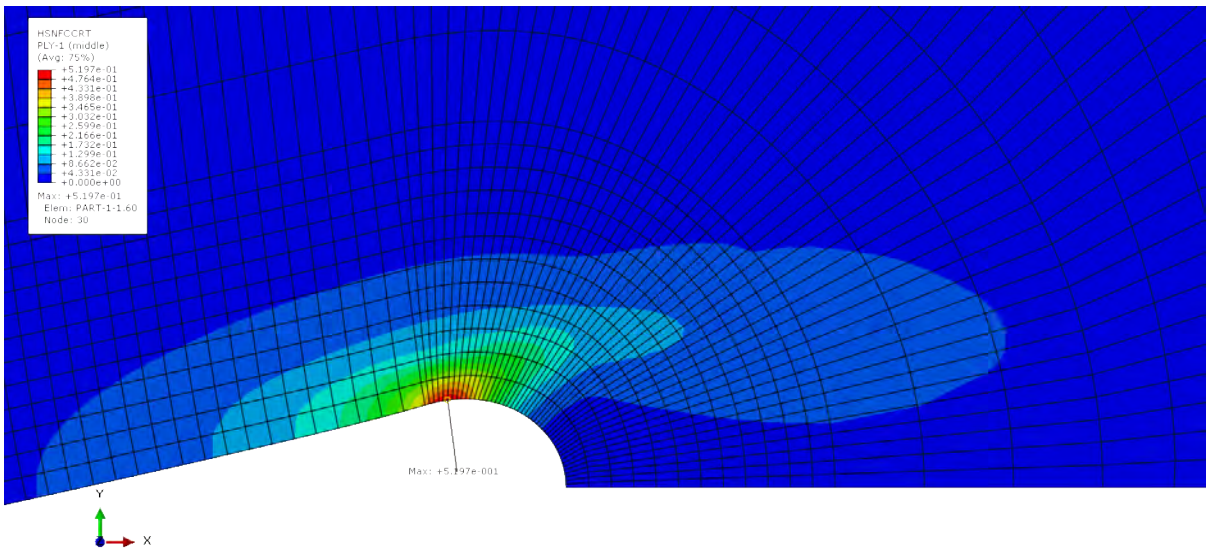

Figure 5.12: Hashin's FC criterion in 90º layer

The behavior of the fibers is interesting to be analyzed. At the moment the experimental specimen undergoes crack propagation for the first time, it can be observed that some of the 0^o-oriented fiber elements have already reached the critical value for Hashin's *Fiber Compression* criterion, following the statement previously proposed that this damage model is very conservative. But if 90^o layers are studied, it can be seen that no element has reach the critical value. A possible explanation for this is that in the modeled specimen, some other important damage modes have been neglected, such as delamination, or any interaction between the matrix cracking and its surrounding fibers. As the model is not experiencing any of this, its fibers are obviously stronger in this 'perfect' environment. A C-scan performed by Pinho in his experimental specimens clearly shows the delamination effects that are been neglected in the FEM model:

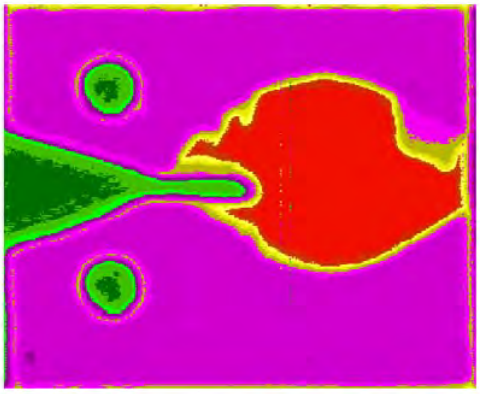

Figure 5.13: Delamination shown in a CC specimen

The effect of the a_0 length on Hashin's *Fiber Compression* mechanism was also studied. Different specimens were modeled, all subject to the same 1-mm displacement. The number of failing elements according to Hashin is compared for each value of a_0, are summarized below. The explanation stated for the CT models (increasing number of failing elements with a_0 due to the use of an average J value) can be used for the CC cases. It is interesting to observe that a similar number of failing elements at the moment of experimental fracture are obtained for both CT and CC simulations, which can be used as validation of the Hashin's theory applied to the studied specimens.

Pre-crack length a_0 (mm)	Failing elements according to Hashin
18	25
19	27
20	27
21	28
22	31
Average no. of failing elements	**27.6**

TABLE 5.2. FC FAILING ELEMENTS AS A FUNCTION OF A_0 LENGTH

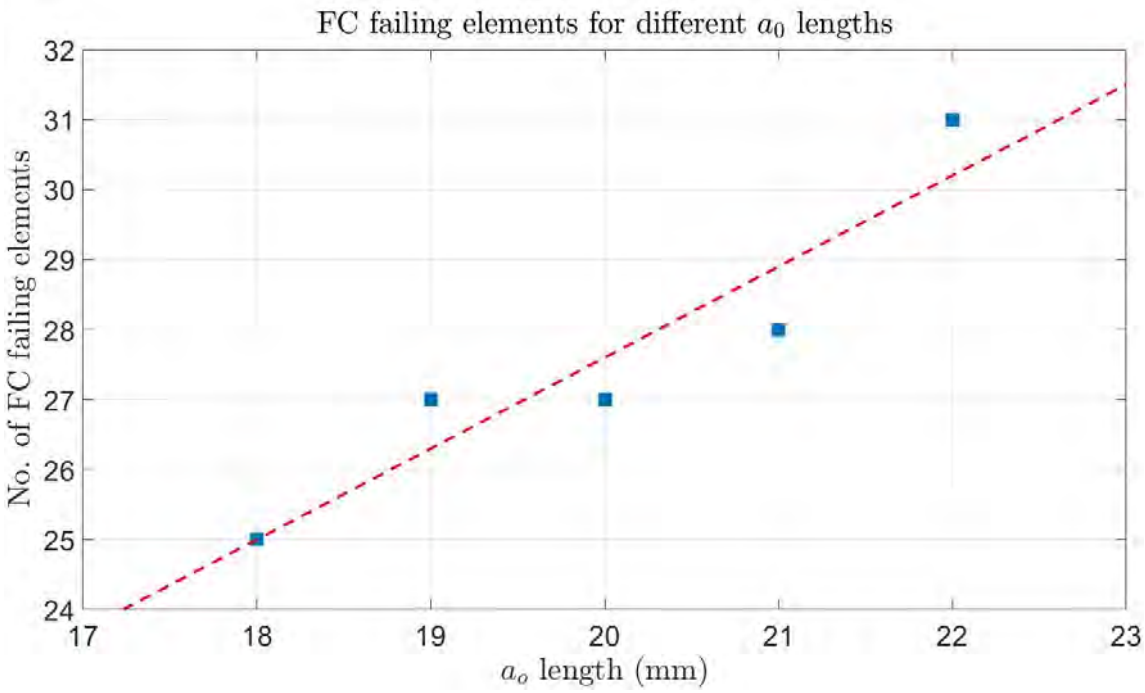

Figure 5.14: FC failing elements as a function of a_0 length

The J curves for different a_0 values show a similar trend to those of the Compact Tension models. Although starting with similar values, as the pin displacement increases it can be seen that those specimens with shorter pre-crack lengths exhibit a steeper energy release rates, due to the higher amount of energy needed to break the larger concentration of fibers and matrix. Compared to the CT results (Figure 5.7), it can be stated that the specimens perform better under tension, as it takes shorter time to reach the experimental critical value for compression, given the same pin displacement.

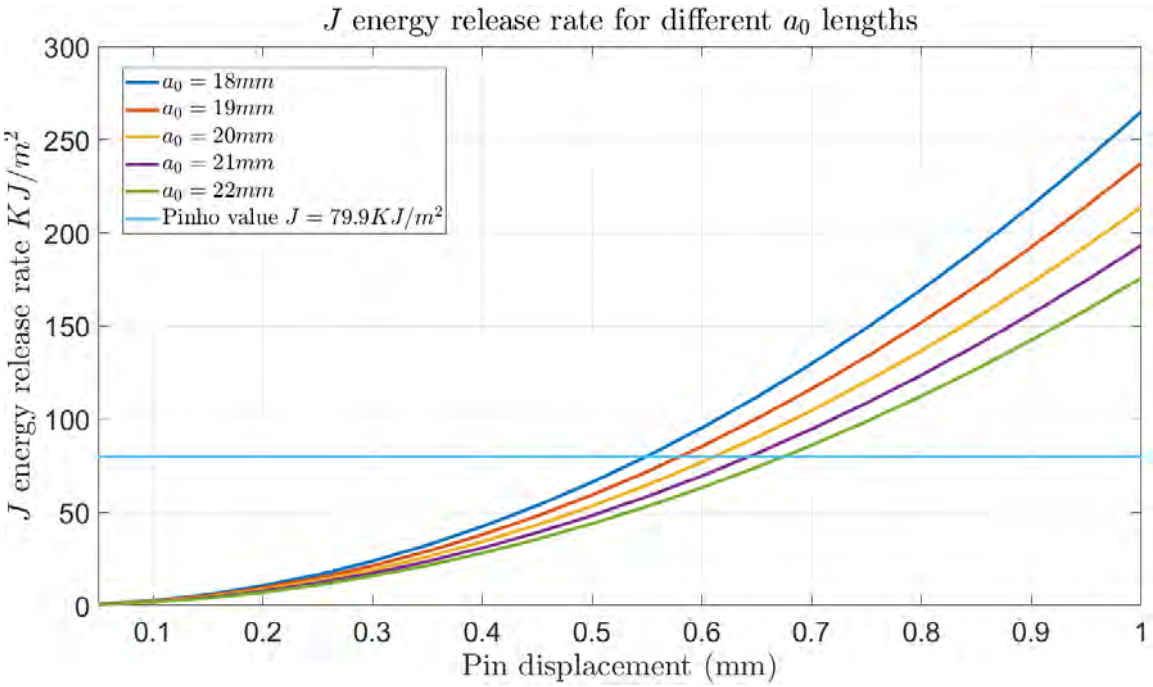

Figure 5.15: J energy release rates for different a_0 values

5.2. Catalanotti's research

The research developed by Catalanotti et al. has as result a new methodology that can be used to determine the compressive crack resistance curve of longitudinal plies of laminate composites. Their developed procedure uses both parametric FEM models and experimental tests, along with the size effect law, to define the resistance curve. The composite of study of the research is IM7-8552, a carbon/epoxy laminate. Using the scaled double-edged notched specimens shown in Figure 4.5, Catalanotti is able to define the value of the steady-state fracture toughness for the IM7-8552 laminate in $\mathbf{61KJ/m^2}$ [13].

This will be the reference value that will be used for this thesis. Following a similar procedure than that of Section 5.1, Hashin's implemented theory is chosen to determine in ABAQUS the fracture energies of the simulated, FEM laminates. Some of the material properties needed for determining Hashin's criteria are not defined in Catalanotti's paper, so once more, the characteristics of the similar AS4-8552 composite studied by Falcó et al. [14] recapped in Table 4.3 are assumed valid for the IM7-8552 laminate.

The first step is to determine the energy release rate curve. Using the contour integral method, a different curve is obtained for each of the contours. It can be seen in Figure 5.16 that the solution quickly converges as even the first contour, normally neglected due to result differences, shows the same trend and values than the other contours.

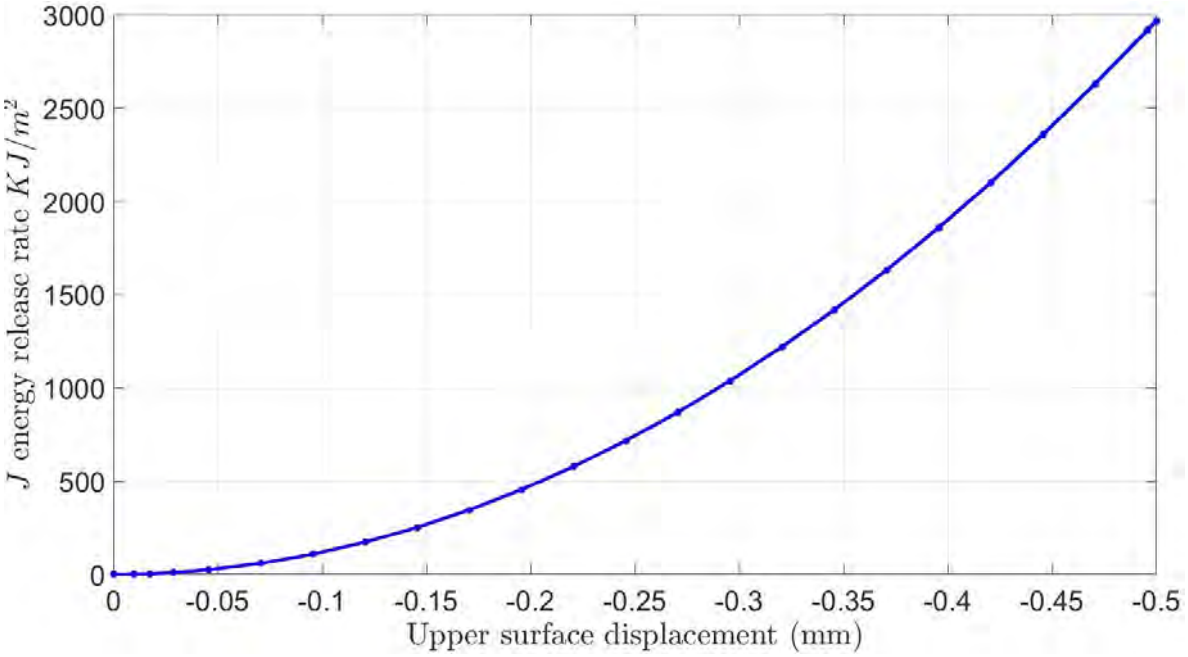

Figure 5.16: Energy release rate contours for A-specimen, under 0.5-mm compression

The experimental value obtained by Catalanotti must be interpreted before its utilization: As only a quarter of the whole specimen geometry is modeled in order to save computational time, ABAQUS only accounts for one crack for its calculations. Given the symmetry of the specimens, an equitable distribution of the specimen's fracture energy among the two cracks can be assumed as reasonable. Therefore, the total $61 KJ/m^2$ value for the laminate can be divided in $30.5 KJ/m^2$ for each of the cracks. This second value is the one used to determine in the J energy release rate curve the moment in time the simulation should have initiated the crack propagation, which will be used to study Hashin's damage mechanisms.

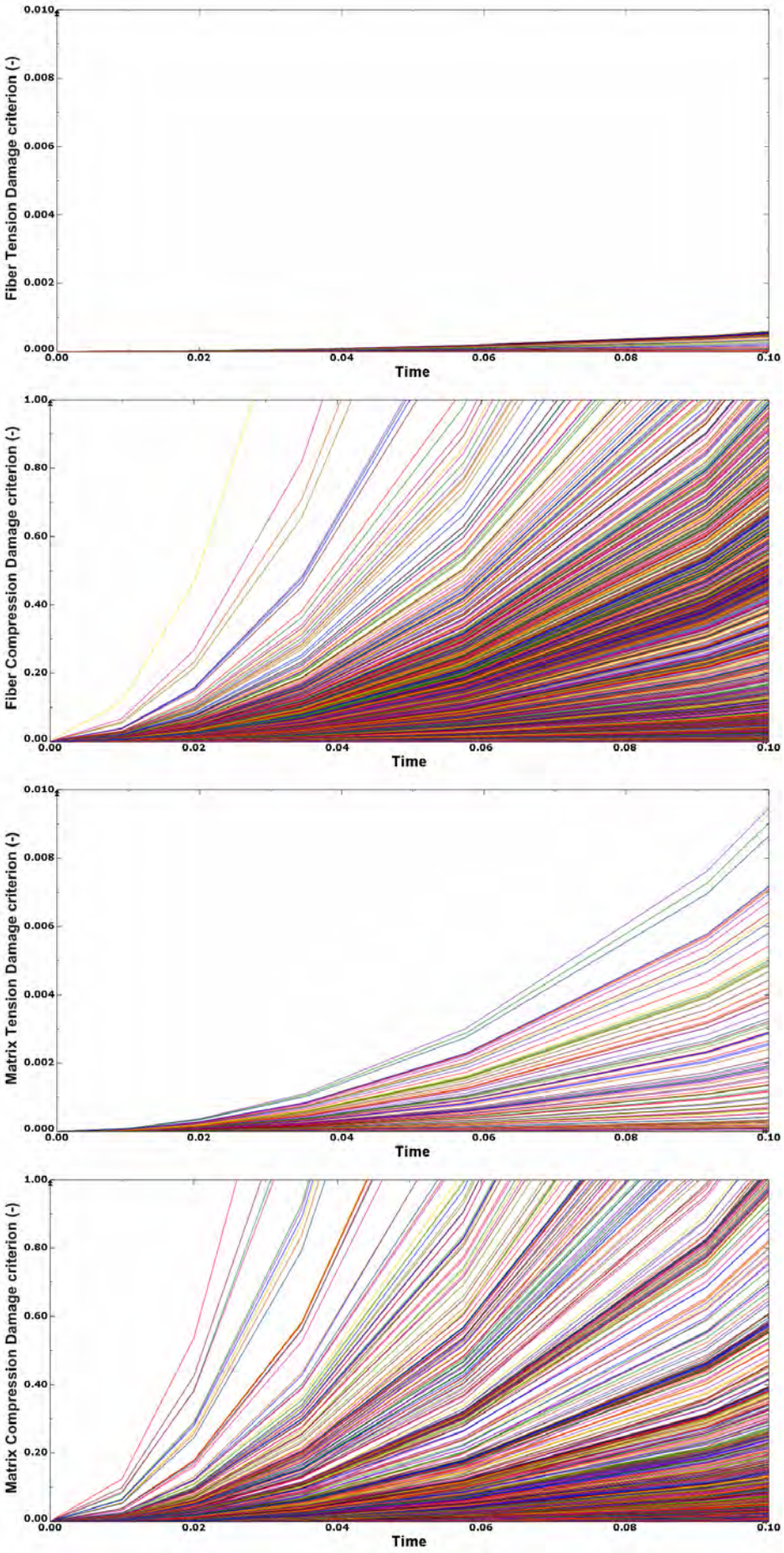

Figure 5.17: Hashin's damage mechanisms - A-specimen, 0º layers

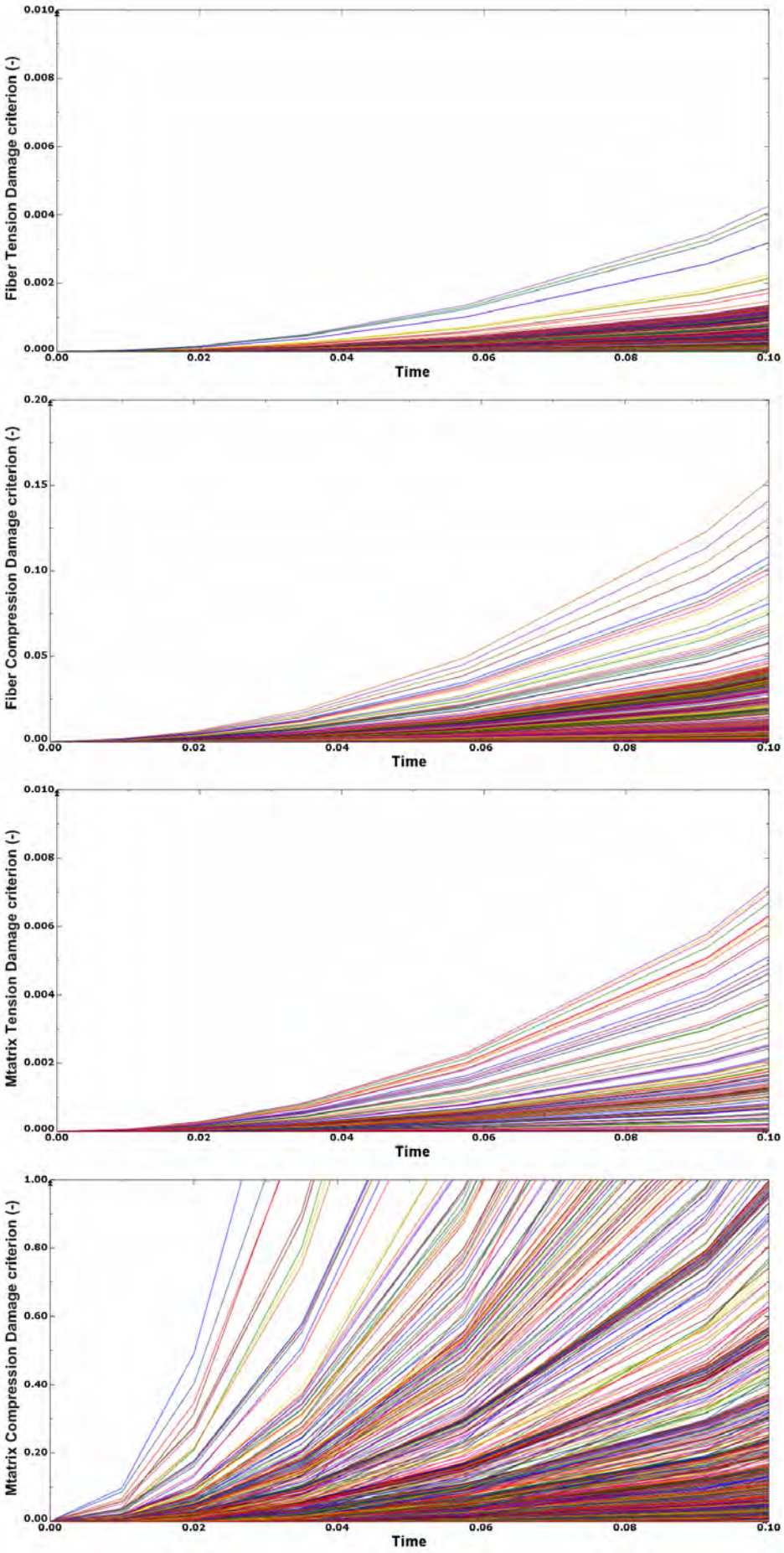

Figure 5.18: Hashin's damage mechanisms - A-specimen, 90º layers

It can be observed that for both orientations, fiber and matrix tension criteria can be perfectly assumed as negligible, as the values obtained are well below 1% of the critical value. A similar trend to that seen in the Compact Compression simulations of Pinho's tests can be appreciated in the 90º layers. At the experimental fracture energy, the Hashin's FC criterion of the fibers contained in these layers are still under the critical value, which means that they have not failed yet. The idealized environment being simulated in ABAQUS, where no other damage modes apart from Hashin's theory is being taken into account, has as result tougher fibers able to withstand larger compression loads than those of the real laminate. Regarding 0º layers, it can seen that a relevant number of elements, located around the crack tip, have failed before the experimental energy release rate value is reached. Hashin's theory is again demonstrated to be a conservative approach, as the laminate is able to withstand larger loads prior to its ultimate failure, which will start the crack propagation.

The contours plotted in Figures 5.19 and 5.20 can be used to visually observe the large differences in terms of absorbed energy by the fibers of the different orientations, and the distribution of failing elements at the moment the laminate would suffer crack propagation using the fracture toughness obtained by Catalanotti:

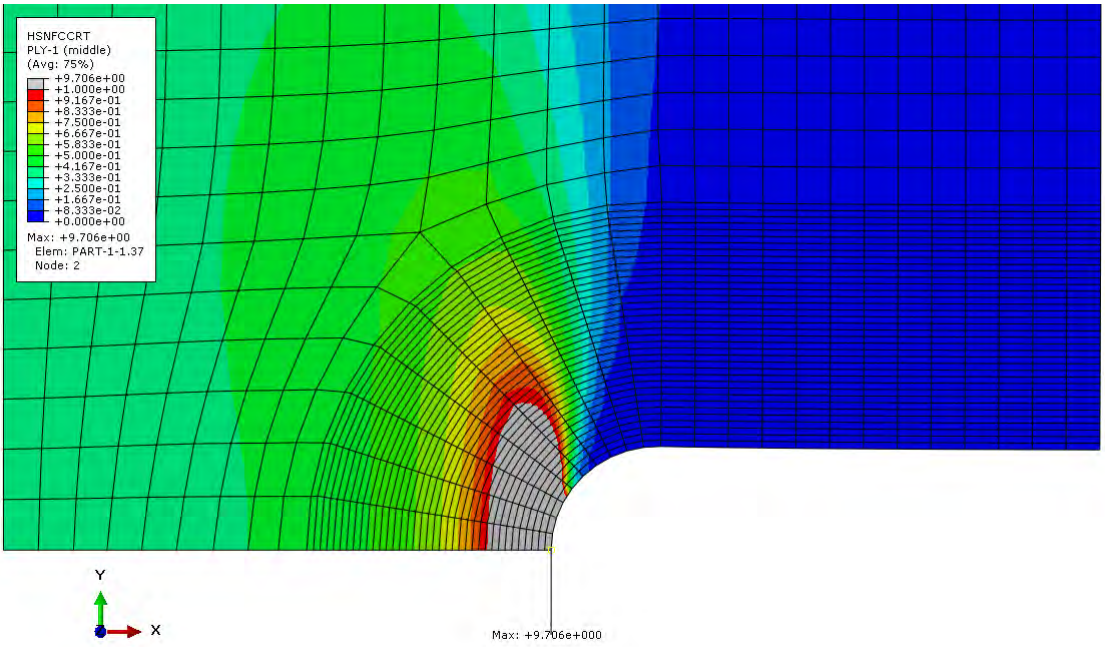

Figure 5.19: Hashin's FC criterion in 0º layer

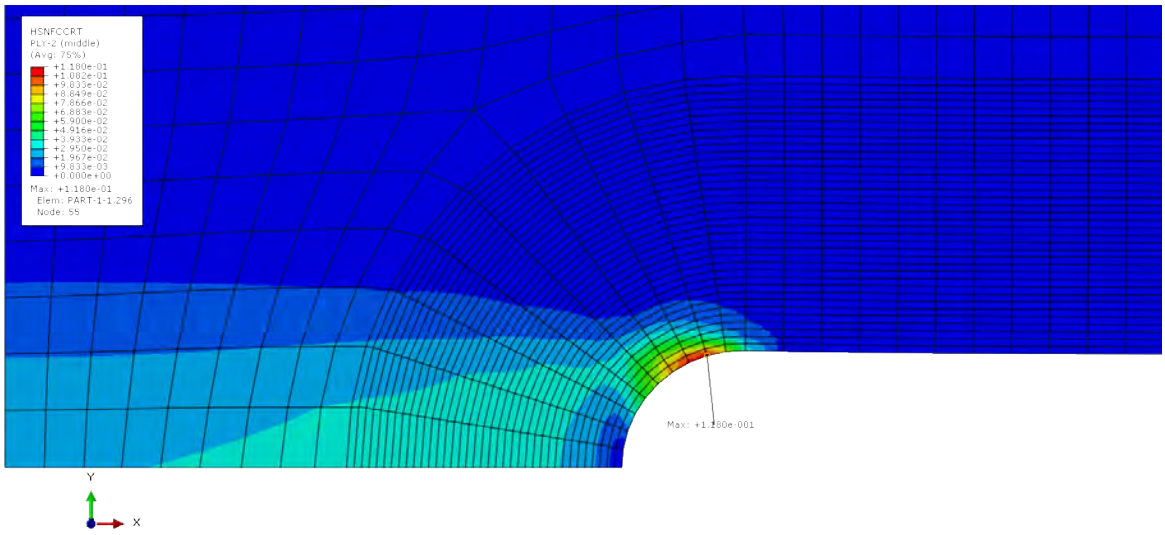

Figure 5.20: Hashin's FC criterion in 90^o layer

D and F specimens (Figure 4.5) were also modeled and simulated, following the procedure stated for the analysis of A specimen. Hashin's damage criteria show a similar trend, being the 0^o, FC criterion the critical one, and the one used to perform a comparison between the different specimens' results, which are summarized in Table 5.3. It can be seen that, despite the difference in size, as the dimensions determining the geometry of the specimens and the crack w and a_o are related by a specified ratio, the results obtained from the simulations can be stated as consistent, validating also the models with the experimental data.

Specimen	*Failing elements according to Hashin*
A	67
D	68
F	76
Average no. of failing elements	**69.3**

TABLE 5.3. FC FAILING ELEMENTS FOR DIFFERENT SPECIMENS

5.3. Effect of alpha coefficient in Hashin's theory

As explained in Section 3.1.1, Hashin's damage model is a very straight-forward method to follow. Simply by using the strength properties of the materials along with the effective stresses acting over a resisting damage area, four damage situations can be differentiated, which can be individually studied. There exists another parameter that has not been explicitly talked about, which is the α coefficient. Hashin uses this parameter to determine how affected is the fiber tension criterion by the shear stress in Equation 3.1. All the results obtained for this Section 5 were obtained by considering the theory originally developed by Hashin and Rotem in 1973 [27] in which $\alpha = 0$ and $S^T = Y^C/2$.

An analysis of the effect of α was found interesting to be performed. The studied specimen is the $a_0 = 26mm$, Pinho's CT laminate, with a 1-mm pin displacement. The results obtained for $\alpha = 0$ stated in Section 5.1 are compared to those obtained for $\alpha = 1$, as stated by Hashin in his 1980's model [28], and an intermediate value $\alpha = 0.5$. The shear stress S^L contribution to the FT criterion is evident, observing Figures 5.21 and 5.22, reducing significantly the time and therefore the needed load, to initially damage the fibers, being seen clearly this phenomenon for the 90º layers. For $alpha = 0$ it is easily observed the difference in the behavior of the 0º and 90º layers, having their first failing element at different moments. As α coefficient is increased, this difference is reduced up to the point in which for $\alpha = 1$ their curves are very similar.

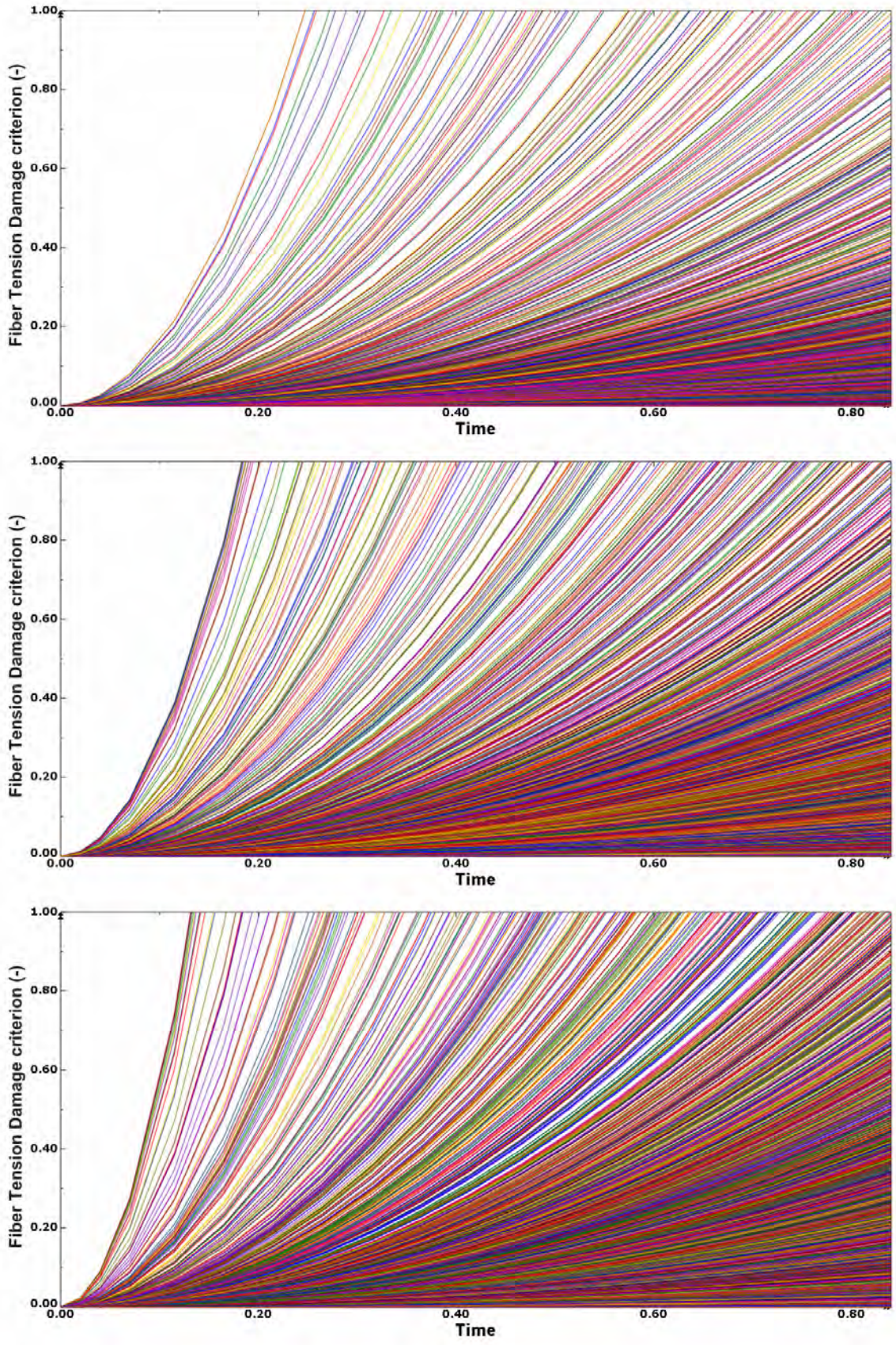

Figure 5.21: 0^o layers, FT criteria for $\alpha = 0$ (up), $\alpha = 0.5$ (middle), $\alpha = 1$ (below)

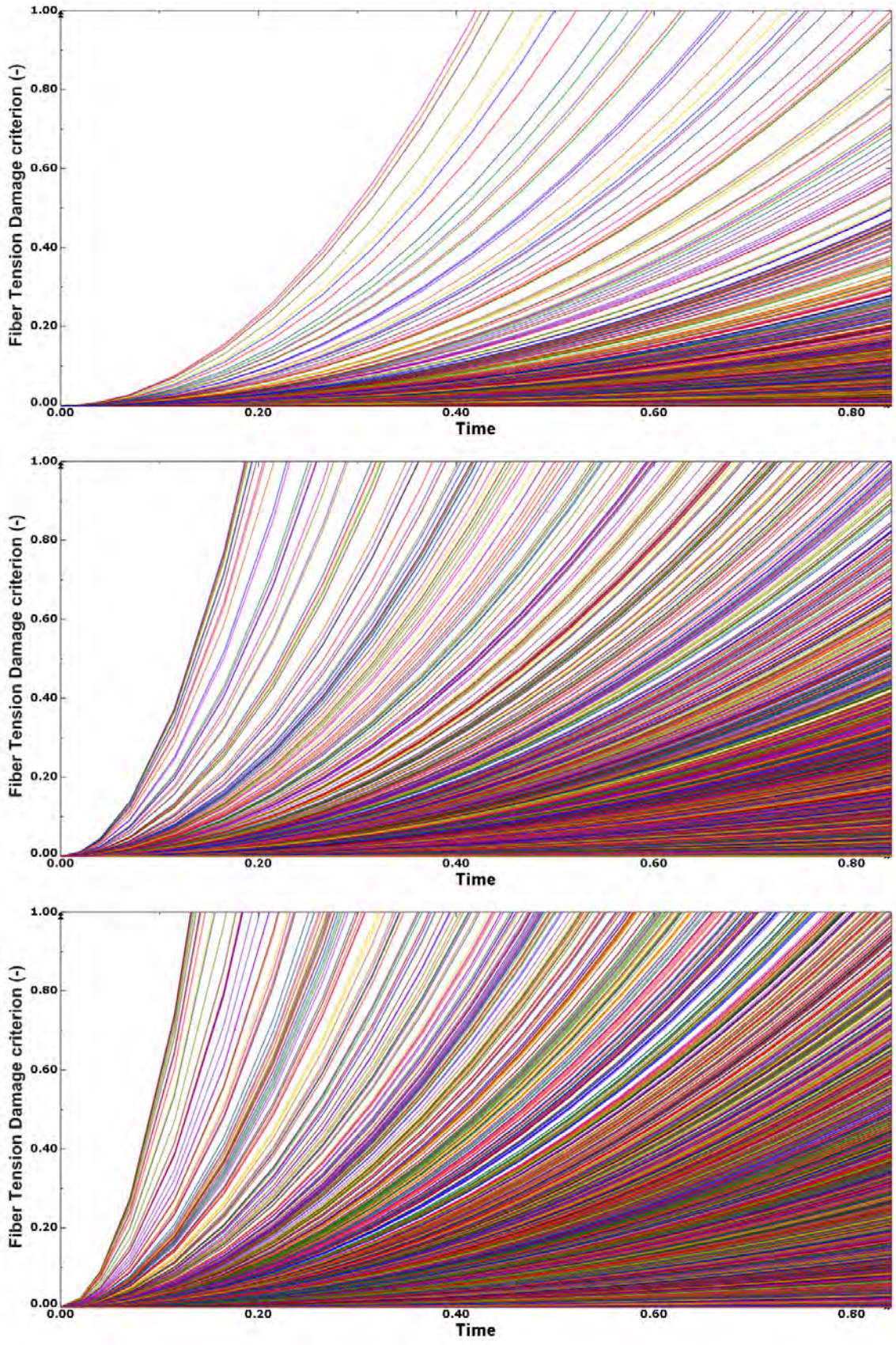

Figure 5.22: 90° layers, FT criteria for $\alpha = 0$ (up), $\alpha = 0.5$ (middle), $\alpha = 1$ (below)

5.4. Comparison of both methodologies

In order to perform a direct comparison of both methodologies, the same material has to be implemented. AS4-8552 composite laminate studied by Falcó et al. [14] will be used, as all the material properties needed by ABAQUS are known. The comparison will be based on the simulations of Pinho's CC specimen with $a_o = 20mm$ and Catalanotti's A specimen.

The procedure followed for this analysis consists on reversing the one used for Sections 5.1 and 5.2: in those Sections, the experimental value for the fracture energy of the laminate was used to determine the number of elements that have failed according to Hashin's damage model before reaching this critical energy value. Now, the average number of failing elements stated in Tables 5.2 and 5.3 is assumed to be the determining parameter. The critical energy release rate will be then calculated from the J-contour curves based on this number. The results obtained are the following:

	Pinho Model	*Catalanotti Model*
Critical energy release rate (KJ/m^2)	**68.6**	**54.2**

TABLE 5.4. CRITICAL ENERGY RELEASE RATE FOR BOTH METHODOLOGIES

Observing the results, it can be stated that, although very different testing dispositions were compared, the fracture energies obtained with both methodologies are relatively similar. This can be considered as a validation of the simulating procedure developed throughout this thesis, even considering all the assumptions that had to be taken in order to be able to elaborate the models with the available resources, ranging from missing material properties to the simplified implemented damage models.

6. SOCIO-ECONOMIC IMPACT AND LEGAL FRAMEWORK

6.1. Socio-economic impact

Throughout the development of this thesis, one of the main advantages of using a FEM software has been repeatedly pointed out: the enormous reduction in cost related to operational costs. Thanks to the unlimited numbers of simulations that the user can perform simply by means of a computer, there is no need to, at least during the first stages of the research, physically manufacture the samples and experimentally test them in a laboratory. Being applicable to every type of material, it is of important relevance for composites, as the raw products and producing processes are generally more expensive than those more traditional materials.

But obviously, there are some costs. Dassault Systèmes, the company behind ABAQUS, has made large investments in developing a fully functional, multi-physics software, that it charges its clients by means of yearly license subscriptions. The person in charge of performing the simulations, including the model implementation and the post-analysis of the results, must also be paid for their job. For all of this, an approximate budget is presented in Table 6.1.

Workforce	
Engineer salary	30€/h
Working hours	300h
Software	
SIMULIA ABAQUS (year license)	30000€
MATLAB (year license)	1000€
TOTAL	**40000€**

TABLE 6.1. ESTIMATED BUDGET

The following Gantt chart illustrates the thesis schedule, specifying the different developed activities and their beginning and ending in time.

Activity	*ID*	*Started*	*Finished*
Background Research	1	feb-18	abr-18
Literature Survey	2	abr-18	ago-18
Model Implementation & Validation	3	may-18	jul-18
Parametric Analysis	4	jul-18	sep-18
Report	5	ago-18	sep-18

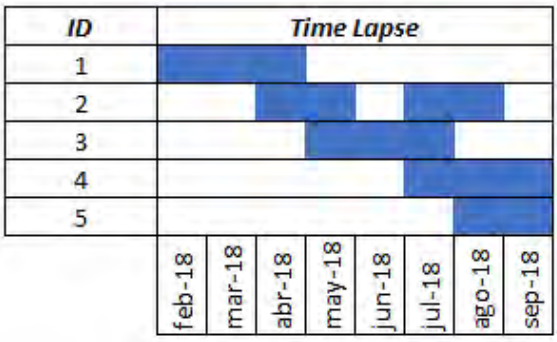

Figure 6.1: Gantt chart

6.2. Legal framework

There exist some standards at the European level that define some basic guidelines in order to guarantee minimum quality levels regarding the manufacturing of composites. The specimens fabricated for the experimental tests used as a basis for this thesis are to follow them. Although the work developed in this report is mostly related to numerical models, they can be assumed also to fulfill the cited standards. As an example, the European standard *ECSS-E-HB-32-20* [29], related to the verification of the manufacturing of composite parts for space projects, can be applied here.

Regarding the FEA software used for the development of this thesis, SIMULIA ABAQUS can be subjected to NAFEMS, the 'International Association for the Engineering Modeling, Analysis and Simulation Community'. This organization, recognized as a valued independent authority in the field, has among its goals, establishing best practice in engineering simulation and promoting the effective use of engineering simulation methods such as finite element analysis.

7. CONCLUSIONS AND FUTURE PROJECTS

7.1. Conclusions

Several numerical models of composite laminates have been implemented in SIMULIA ABAQUS, with the objective of accurately simulating some Compact Tension and Compression tests. The results obtained with the FEM models have been compared to the experimental ones. The corresponding analysis drew the following conclusions:

- ABAQUS offers an easy and intuitive method to simulate composite layups. Defining some elemental material properties, an interesting range of parameters can be studied.
- The simpleness of the available composite laminate simulation has as drawback that some other important damage modes, like delamination, are absent from the calculations, which may have a relevant impact on the obtained results.
- Hashin's implemented theory has been shown to be a conservative approach, in terms of crack initiation energies. If a strict interpretation of his damage model was to be used, the obtained energies would be significantly lower than the experimental ones.
- ABAQUS/Implicit is unable to perform element removal, reducing the operational effectiveness of the models to the initiation of the crack.
- With the available material properties, the composite material had to be modeled as perfect elastic. For this reason, the experimental value obtained for crack initiation energy is needed to perform the corresponding analysis.
- For all the previous statements, the implemented FEM models can be used as a first, easy-to-use introduction to the world of composite simulations using FEA software. If experimental values are also available, the models can also be useful for result verification. Nevertheless, the simulations have proved to be consistent and the results to be accurate enough.

7.2. Future projects

Some ideas are here listed that could be use to continue the developed work in this thesis that could yield more accurate results and therefore, a more precise representation of the reality:

- The use of other fracture mechanics methods that are being implemented in ABAQUS, like the eXtended Finite Element Method (XFEM), could yield more precise and independent results, not only for crack initiation but also propagation. An interesting relationship between the crack size a and the specimen width w could be analyzed.
- Some optional parameters needed by the Hashin's implemented model, such as ply fracture energies and viscosities, could be defined in ABAQUS to automatically obtain the critical initiation energy release rate. The material had to be firstly tested in the laboratory to determine these properties.
- The behavior of the cohesive layer could also be simulated and analyzed, in order to determine how the obtained results would be affected by the addition of this new element.
- Other FEA software like LS-DYNA could be used to simulate the same models, and a comparison between the results would yield interesting conclusions to determine which available commercial software performs a more accurate composite simulation, based on different parameters like computational time cost.

BIBLIOGRAPHY

[1] I. M. Daniel and 0. Ishai. *Engineering Mechanics of Composite Materials*. 1st ed. New York: Oxford University Press. Inc, 1994.

[2] Oxyblack, *Laminates & Sandwiches*, 2017. [Online]. Available at https://www.oxyblack.com/images/Composites/Fibers-orientation.png

[3] ASM International. *ASM Handbook Volume 21: Composites* 1st ed. Materials Park, OH: ASM International, 2001.

[4] Aennova, *Tecnologías de Composites*, 2014. [Online]. Available at http://www.aernnova.com/es/actividades/composites/tecnologias-de-composites/

[5] Nuplex, *Filament winding*, 2014. [Online]. Available at http://www.nuplex.com/composites/processes/filament-winding

[6] Nuplex, *Resin transfer moulding*, 2014. [Online]. Available at http://www.nuplex.com/composites/processes/resin-transfer-moulding

[7] Creative Pultrusions, *Fiberglass Pultrusion Process*, 2016. [Online]. Available at https://www.creativepultrusions.com/index.cfm/products-solutions/fiberglass-pultrusion-process/

[8] 'Team New Zealand confirms next Americas Cup in Monohulls', *Catamaran Racing, news and design*, 11-09-2017 [Online]. Available at https://www.catsailingnews.com/2017/09/team-new-zealand-confirms-next-americas.html

[9] NASA, *Spacecraft icons*, 2017. [Online]. Available at https://science.nasa.gov/toolkits/spacecraft-icons

[10] BAE Systems, *Eurofighter Typhoon - The European solution*, 2017. [Online]. Available at https://www.baesystems.com/en-be/campaign-typhoon-for-belgium/the-european-solution

[11] F. Raddatz, *Faserverbundstoffe in der Luftfahrt*, Deutsches Zentrum für Luft- und Raumfahrt, 2015.

[12] S. Pinho, P. Robinson and L. Iannucci, "Fracture toughness of the tensile and compressive fibre failure modes in laminated composites", *Composites Science and Technology*, vol. 66, no. 13, pp. 2069-2079, 2006.

[13] G. Catalanotti, J. Xavier and P. Camanho, "Measurement of the compressive crack resistance curve of composites using the size effect law", *Composites Part A: Applied Science and Manufacturing*, vol. 56, pp. 300-307, 2014.

[14] O. Falcó, R. Ávila, B. Tijs and C. Lopes, "Modelling and simulation methodology for unidirectional composite laminates in a Virtual Test Lab framework", *Composite Structures*, vol. 190, pp. 137-159, 2018.

[15] W.C. Jackson and J.G. Ratcliffe, "Measurement of fracture energy for kinkband growth in sandwich specimens", (paper no. 24). *Composites testing and model identification, CompTest2004*, 2004.

[16] R.D. Cook, D.S. Malkus and M.E. Plesha, *Concepts and Applications of Finite Element Analysis*. 3rd ed. New York: John Wiley and Sons, 1989.

[17] R.B. Deo, J.H. Starnes and R.C. Holzwarth, “Low-cost composite materials and structures for aircraft applications”, in *RTO AVT Specialists’ Meeting on “Low Cost Composite Structures”*, 2001.

[18] ESA, *The XMM-Newton Spacecraft*, 2016. [Online]. Available at https://www.cosmos.esa.int/web/xmm-newton/technical-details-spacecraft

[19] R.Lukez, “The use of graphite/epoxy composite structures in space applications”, in *AIAA/USU Conference on Small Satellites*, 1987. [Online] Available: https://digitalcommons.usu.edu/smallsat/1987/all1987/12/

[20] S. Selvaraju "Applications of composites in marine industry", *Journal of Engineering Research and Studies*, vol. 2, pp 89-91, 2011.

[21] Saleh R. Abdussalam, *Damage and fracture mechanics of composite materials*, PhD thesis, University of Manitoba, Winnipeg, Manitoba, Canada, 1999. [Online]. Available at http://hdl.handle.net/1993/2148

[22] Thomas J. Wright, *Sensitivity of Hashin damage parameters for notched composite panels in tension and out-of-plane bending*, MSc thesis, Oregon State University, Corvallis, Oregon, USA, 2012. [Online]. Available at https://ir.library.oregonstate.edu/downloads/xg94ht47t

[23] S. Peters, *Handbook of Composites*. 2nd ed. London: Chapman & Hall, 1998.

[24] W. Callister, *Materials Science and Engineering. An Introduction*. 7th ed. John Wiley and Sons, 2006.

[25] T.L. Anderson. *Fracture Mechanics: Fundamentals and Applications*. 3rd ed. Boca Raton, FL: CRC Press, 2005.

[26] *ABAQUS 6.14 Analysis/CAE Guide*. Dassault Systèmes, 2014.

[27] Z. Hashin and A. Rotem, "A Fatigue Failure Criterion for Fiber Reinforced Materials", *Journal of Composite Materials*, vol. 7, no. 4, pp. 448-464, 1973.

[28] Z. Hashin, "Failure Criteria for Unidirectional Fiber Composites", *Journal of Applied Mechanics*, vol. 47, no. 2, pp. 329-334, 1980.

[29] *Structural materials handbook*, ECSS-E-HB-32-20, 2011.